Tools for understanding the glycosaminoglycan biosynthesis

Willén, Daniel

2021

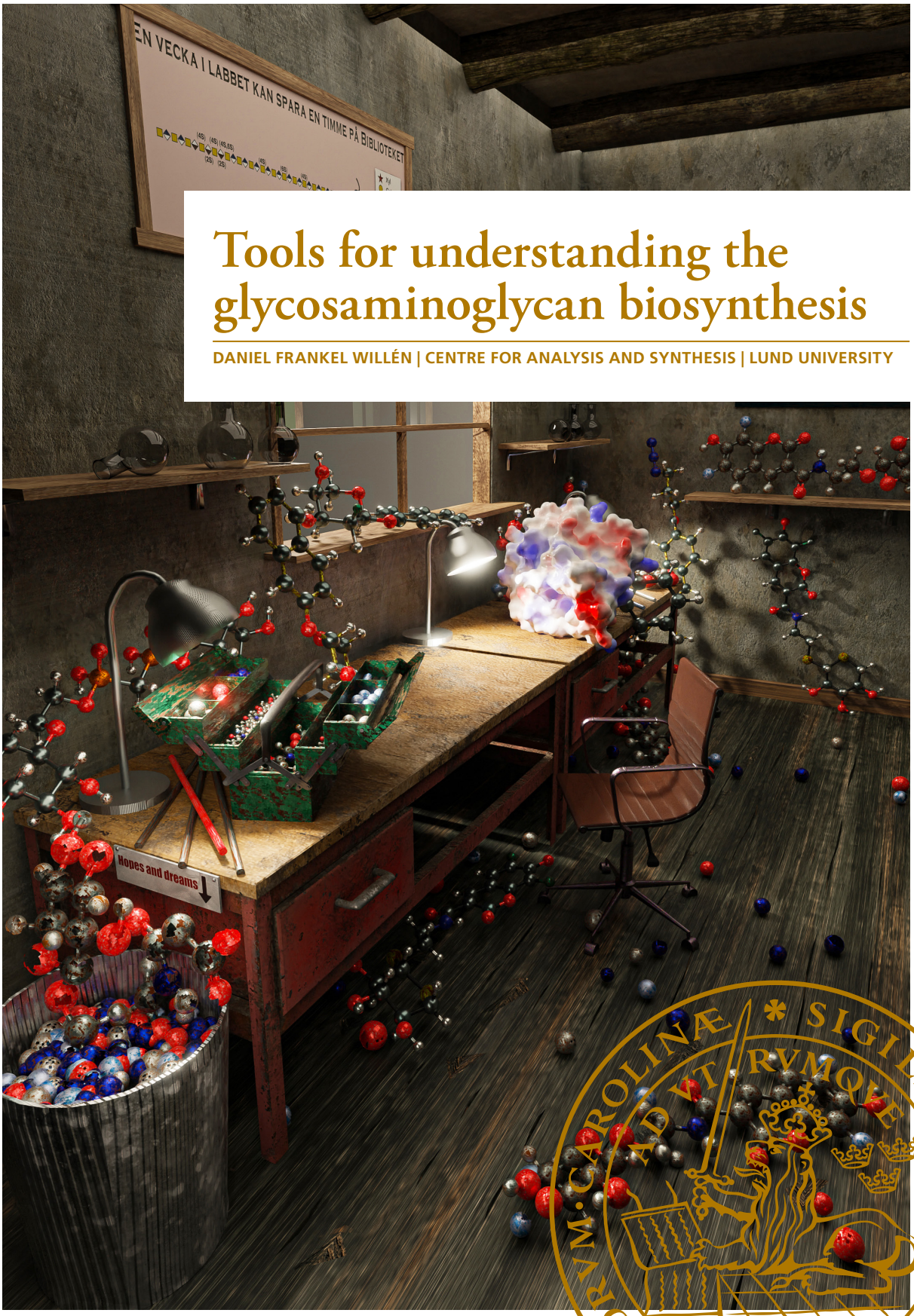

Tools for understanding the glycosaminoglycan biosynthesis

DANIEL FRANKEL WILLÉN | CENTRE FOR ANALYSIS AND SYNTHESIS | LUND UNIVERSITY

Printed by Media-Tryck, Lund 2021 NORDIC SWAN ECOLABEL 3041 0903

LUND UNIVERSITY

ISBN 978-91-7422-846-5

Centre for Analysis and Synthesis
Department of Chemistry
Faculty of Science
Lund University

Tools for understanding the glycosaminoglycan biosynthesis

Tools for understanding the glycosaminoglycan biosynthesis

by Daniel Frankel Willén

LUND
UNIVERSITY

Thesis for the degree of Doctor of Philosophy

Thesis advisors:	Prof. Ulf Ellervik Dr. Sophie Manner
Faculty opponent:	Prof. Stefan Oscarson

To be presented, with the permission of the Faculty of Science of Lund University, for public criticism at Kemicentrum (Hall B) on Thursday, the 2nd of December 2021 at 09.00.

Organization	Document name
LUND UNIVERSITY Department of Chemistry Box 124 SE–221 00 LUND Sweden	**DOCTORAL THESIS** Date of disputation 2021-12-02 Sponsoring organization
Author(s) Daniel Frankel Willén	

Title and subtitle

Tools for understanding the glycosaminoglycan biosynthesis

Abstract

For cells to function correctly within an organism, they need different systems to communicate with each other. One crucial part of cell signaling is the proteoglycans (PGs) and glycosaminoglycans (GAGs), which are macromolecules that bind different signaling molecules and proteins necessary for processes such as growth and proliferation. Therefore, PGs and GAGs are involved in pathological processes like cancer and bacterial or viral infection. A tetrasaccharide linker connects several types of GAGs to the PG core protein, with the first carbohydrate being a xylose. Xylose is, due to its scarcity in mammalian cells, an attractive target for therapeutics. In GAG biosynthesis, the enzyme β4GalT7 galactosylates the xylose. Therefore, this enzyme could be interesting to target using synthetic xylosides that could act as substrates or inhibitors. These xylosides could allow us to understand and control the biosynthesis of GAGs.

This thesis is focused on the design and synthesis of modified xylosides and how we can use these as tools to study the formation of GAGs. We decided to alter the carbohydrate itself to investigate if it is possible to design effective substrates or inhibitors for β4GalT7. We also decided to modify the aglycon, the part attached to the carbohydrate, to answer questions related to how cells process GAGs. This work has resulted in several new substances that, that enter cells, and work well as substrates and inhibitors of β4GalT7 to provide answers to how GAGs are structured, how they move within the cell, and how they interact with other biomolecules such as viral proteins. The results of this work pave the way for the use of synthetic xylosides to answer several questions about GAG-related processes and open up the possibility for creating tools for influencing and studying cells' expression of GAGs.

Key words

xylosides, glycosaminoglycans, proteoglycans, β4GalT7, carbohydrate synthesis, GAG priming, GAG inhibition

Classification system and/or index terms (if any)

Supplementary bibliographical information	Language
	English
ISSN and key title	ISBN
	978-91-7422-846-5 (print) 978-91-7422-847-2 (pdf)
Recipient's notes	Number of pages: 204 / Price
	Security classification

Tools for understanding the glycosaminoglycan biosynthesis

by Daniel Frankel Willén

LUND
UNIVERSITY

Author photo: Picture by Rebecca Frankel Willén

Quote: Dara Ó Briain, Dara Ó Briain Talks Funny: Live in London, 2008

Cover illustration front: by Thomas Willén.

Cover illustration back: by Daniel Frankel Willén.

Faculty of Science, Department of Chemistry

ISBN: 978-91-7422-846-5 (print)
ISBN: 978-91-7422-847-2 (pdf)

Printed in Sweden by Media-Tryck, Lund University, Lund 2021

Printed matter
3041 0903

Media-Tryck is a Nordic Swan Ecolabel certified provider of printed material. Read more about our environmental work at www.mediatryck.lu.se

MADE IN SWEDEN

People say "Science doesn't know everything!"
— Science knows it doesn't know everything, otherwise it'd stop.

Contents

Acknowledgements

The destination is only one part of the journey. And I would certainly not be where I am today without numerous people I have met along the way. How does one person express so much gratitude in only a couple of pages? I do not know, but I will try my best!

Firstly, I'd like to express my sincerest thankfulness to **Ulf**. I consider myself extremely honored to have been part of your research group and for this opportunity to be part of such an exciting field of research. Also, I am eternally grateful for the chance to participate in *Fråga Lund* and *Kemishowen*; I've learned so much from that as well. Your enthusiasm is truly inspiring, and I'll forever cherish the moments we've had during these almost seven years together.

Secondly, **Sophie**, I would like to thank you for always being supportive, encouraging, and an overall fantastic person. Even though you have been incredibly busy, it has always been possible to talk with you regarding everything from research, teaching, and life outside of academia. You are genuinely an idol when it comes to science.

Thank you to Group UE, past and present. Especially **Karin** for being my supervisor when I just arrived as a master student, **Emil** for being a fantastic scientist and all-around good guy (I still think we would not have gotten anything done if we were to share a lab), and **Andrea** for being an absolute professional. I also appreciate all my diploma workers who have aided me, even if just a little.

I am very grateful to all terrific PhD colleagues at CAS —past and present— for making the workplace great. An honorable mention to **Tiago**, for being a genuine friend and awesome lab mate; **Roberto**, for all the silly memes and your easy-going attitude; **Alexander D**, for your endless ramblings, general knowledge, and being a member of the Superbock dream-team, **Valtyr**, and **Samuel**, for being KEMA01 brothers-in-arms (snilld!); **Maria-Luisa**, for good stories and keeping the food-standard high; **Aleksandra**, for your front-cover quote suggestion; **Anna**, **Lisa**, **Jesper**, **Mujtaba**, **Vicky**, **Niels**, and **Simon**, for the sweat and tears in the synthesis course, teaching labs and laughs in the lunchroom.

Also, I would like to thank the seniors and admin at CAS for making it such a great working place. Especially **Maria L**, for keeping CAS afloat as well as your some-good-some-bad puns; **Katarina**, for always going the extra mile when asked for help; **Sofia**, for all the MS-analysis and answering my silly questions; **Peter Somfai**, for putting so much trust in my teaching skills in KEMA01.

I'd also like to thank all of the people I have collaborated with during my PhD studies for the opportunity to do science together.

All my friends from my study time at Linköping University: **Maccan**, **Maja**, **Carl**, **Fredrik**, **Ulrika**, **Linnea**, **Elin**, **Louise**, **Sofie A**, **Kvarnen**, **Cassman**, **Malin L**, **Malin G**, **Bullen**, **William**, **Josef**, **Johanna**, **Ronja**, **Mattias**, **Måns**, **Johnny**, **Fanny**, **Elisabeth**, **Sandra** and more. You indeed are one of the most wonderful bunch of people I know. The memories of our events, travels, parties, and across-the-board ridiculous things we experienced are memories I will cherish forever.

Anton, **Joakim**, and **Niklas**, my lifelong friends from Västerås. Your loyalty over the years has been unmatched.

My incredible family (even though you barely had a clue about what I was doing): Mom and Dad —**Maria** and **Olle**—, my Sister **Malin**, and my Grandparents — **Lennart**, **Iréne**, **Gun**, and **Hans**— for the huge amount of support and love throughout the years, I could not have wished for a better family. I love you immensely. Thank you, Uncles and Cousins with their spouses, particularly **Thomas**, for the fantastic job with the front cover. My in-laws: **Lotta**, **Krister**, **Sandra**, **Jonatan**, **Simone**, **Natali**, and **Ronja**, for being an awesome second family.

Momo, our cat, for being the cutest fluff-ball I have ever met and properly converting me into the cat-person I am today. I can always count on you showing up being adorable when I need it.

Finally, thank you to my extraordinary wife, **Rebecca**. For all the moments of joy and frustration, and ups and downs during our journeys as PhDs together. It is truly a privilege to spend my days with such an astounding, intelligent, and down-to-earth person. All the love in the world to you. Du är bäst.

List of publications

This thesis is based on the following publications, referred to by their Roman numerals:

I **Naphthyl Thio- and Carba-xylopyranosides for Exploration of the Active Site of β-1,4-Galactosyltransferase 7 (β4GalT7)**
Thorsheim, K., **Willén, D.**, Tykesson, E., Ståhle, J., Praly, J-P., Vidal, S., Johnson, M T., Widmalm, G., Manner, S., Ellervik, U
Chemistry - A European Journal, **2017**, *23* (71), pp. 18057-18065

II **Synthesis of Double-Modified Xyloside Analogs for Probing the β4GalT7 Active Site**
Willén, D., Bengtsson, Dennis., Clementson, S., Tykesson, E., Manner, S., Ellervik, U.
Journal of Organic Chemistry, **2018**, *83* (3), pp. 1259–1277

III **LC-MS/MS Characterization of Xyloside-primed Glycosaminoglycans with Cell-specific Cytotoxic Properties Reveals Structural Diversity and Novel Glycan Modifications**
Persson, A, Gomez Toledo, A., Vorontsov, E., Nasir, W., **Willén, D**., Noborn,F., Ellervik, U., Mani, K., Nilsson, J., Larson, G.,
Journal of Biological Chemistry, **2018**, *293* (26), pp. 10202-10219

IV **The GAGOme: a cell-based method for display of glycosaminoglycans**
Chen, Y-H., Mao, Y., Narimatsu, Y., Clausen, T., Gomes, C., Karlsson, R., Steentoft, C., Spliid, C., Gustavsson, T., Salanti, A., Persson, A., Malmström, A., **Willén, D**., Ellervik, U., Bennett, E., Yang, Z.
Nature Methods, **2018**, *15* (11), pp. 881-888

V **Fluorescently labeled xylosides provides insight in the biosynthetic pathways of glycosaminoglycans**
Mastio, R.†, **Willén, D.**†, Söderlund, Z., Westergren-Thorsson, G., Manner, S., Tykesson, E., Ellervik, U.
Submitted

VI **An azide functionalized naphthoxyloside as a tool for glycosaminoglycan investigations**
Willén, D., Mastio, R., Söderlund, Z., Manner, S., Westergren-Thorsson, G., Tykesson, E., Ellervik, U.
Submitted

VII **Inhibition of the glycosaminoglycan biosynthesis: Exploration of the binding pocket of β4GalT7 by phoshonate-xyloside constructs**
Willén, D., Malmquist, H., Blasco, P., Björklund, J., Manner, S., Widmalm, G., Tykesson, E., Ellervik, U.
Manuscript in preparation

† These authors contributed equally to this work

My contributions to the papers

Paper I: Naphthyl Thio- and Carba-xylopyranosides for Exploration of the Active Site of β-1,4-Galactosyltransferase 7 (β4GalT7)

I synthesized and characterized the majority of the compounds. I also contributed to the interpretation of data, and writing, editing, and illustrating the manuscript.

Paper II: Synthesis of Double-Modified Xyloside Analogs for Probing the β4GalT7 Active Site

I synthesized and characterized the majority of the compounds. I also contributed to writing, editing, and illustrating the manuscript.

Paper III: LC-MS/MS Characterization of Xyloside-primed Glycosaminoglycans with Cell-specific Cytotoxic Properties Reveals Structural Diversity and Novel Glycan Modifications

I synthesized and characterized the compounds. I also contributed to writing, editing, and illustrating the manuscript.

Paper IV: The GAGOme: a cell-based method for display of glycosaminoglycans

I synthesized and characterized the compounds. I also contributed to writing, and editing the manuscript.

Paper V: Fluorescently labeled xylosides provides insight in the biosynthetic pathways of glycosaminoglycans

I contributed to the formulation of the research question. In addition, I supervised the synthesis and characterization of the compounds. I also contributed to the interpretation of data, and writing, editing, and illustrating the manuscript.

Paper VI: An azide functionalized naphthoxyloside as a tool for glycosaminoglycan investigations

I contributed to the formulation of the research question. I synthesized and characterized the majority of compounds. I also contributed to interpretation of data, and writing, editing, and illustrating the manuscript.

Paper VII: Inhibition of the glycosaminoglycan biosynthesis: Exploration of the binding pocket of β4GalT7 by phoshonate-xyloside constructs

I contributed to the formulation of the research question. In addition, I synthesized and characterized the compounds. I also contributed to the interpretation of data, and writing, editing, and illustrating the manuscript.

Populärvetenskaplig sammanfattning på svenska

Lika mycket som vi människor behöver kunna kommunicera med varandra, måste kroppens celler göra det. Cellerna har därför flera olika system för att signalera till sin omgivning. En viktig del av signalsystemet är *proteoglykanerna* som är proteiner som har långa kedjor av kolhydrater kopplade till sig. Dessa kedjor kallas *glykosaminoglykaner*, och har bland annat till uppgift att fånga in och binda olika signalsubstanser och signaleringsproteiner som har betydelse för cellens tillväxt och utveckling. Detta system är därför väsentligt vid olika sjukdomsförlopp såsom cancer och COVID-19.

Flera typer av GAGs är kopplade till proteinet med en kedja som består av fyra kolhydrater, varav den första är en sockerenhet som heter *xylos*. Denna kolhydrat är ganska ovanlig i däggdjursceller. Det är sedan tidigare känt att man kan göra konstgjorda *xylosider*, det vill säga xylos kopplad till någon annan molekyl, som kan ta sig in i cellen och antingen starta eller blockera bildandet av GAGs. Detta sker genom att xylosiderna binder till β4GalT7, det enzym som kopplar nästa kolhydrat (en galaktos) i kedjan. Eftersom det är ett tidigt steg i syntesen av GAGs kan xylosider användas för att förstå och styra biosyntesen.

Denna avhandling handlar om design och syntes av konstgjorda xylosider och hur dessa kan användas som verktyg för att studera bildandet av GAGs. Vi har valt att modifiera själva kolhydraten för att undersöka hur känsligt β4GalT7 är för förändringar och ifall det är möjligt att designa bra substrat eller hämmare för enzymet. Dessutom har vi arbetat med att modifiera xylos med olika *aglykon* (delen som är kopplad till kolhydraten) för att få svar på frågor som är relaterade till hur cellen behandlar GAGs. Detta har resulterat i flera nya substanser som dels fungerar bra som substrat samt hämmare för β4GalT7, och dels kan gå in i celler och ge svar på hur GAGs är uppbyggda, hur de rör sig inom cellen samt hur de interagerar med andra biomolekyler såsom virusproteiner.

Resultaten i denna avhandling banar väg för att använda syntetiska xylosider för att få svar på ett antal frågor om GAG-relaterade processer samt öppnar upp för att skapa verktyg för att påverka och studera cellers uttryck av GAGs.

Abbreviations

2,2,3,3-TMB	2,2,3,3-tetramethoxybutane
A549 cells	Adenocarcinomic human alveolar basal epithelial cells
AIBN	Azobisisobutyronitrile
BDA	Butane-2,3-diacetal
BODIPY	Dipyrromethene boron difluoride
CSA	Camphorsulfonic acid
CCD-1095Sk cells	Human breast fibroblast cell line
DAST	Diethylaminosulfur trifluoride
DBU	1,8-Diazabicyclo[5.4.0]undec-7-ene
DIAD	Diisopropyl azodicarboxylate
DIPEA	N,N-Diisopropylethylamine
DMAP	4-Dimethylaminopyridine
DS	Dermatan sulfate
ECM	Extracellular matrix
EDC	1-Ethyl-3-(3-dimethylaminopropyl)carbodiimide
EDS	Ehler-Dahnlos syndrome
ER	Endoplasmatic reticulum
GAG	Glycosaminoglycan
HCC70 cells	Human breast carcinoma cell line
HGF	Hepatocyte growth factor
HOBt	Hydroxybenzotriazole
HS	Heparan sulfate
KS	Keratan sulfate
LC-MS/MS	Liquid chromatography-tandem mass spectrometry
PacBlue	3-carboxy-6,8-difluoro-7-hydroxycoumarin
PG	Proteoglycan
Phth	Phthalimide
PTC	Phase-transfer catalysis
SPR	Surface plasmon resonance
TBAB	Tetrabutylammonium bromide
$TBAHSO_4$	Tetrabutylammonium bisulfate
TBDMS	*tert*-Butyldimetylsilyl
OTf	Trifluoromethanesulfonate
TGF-β	Transforming growth factor beta
TNF-α	Tissue necrosis factor alpha

Abbreviations found in the ACS Style Guide is not included.

The most fundamental and lasting objective of synthesis
is not production of new compounds, but production of properties.
— George S. Hammond

Chapter 1

Introduction

1.1 Cellular signaling

All life consists of cells, and they are not solitary organisms; they exist in a continuously changing environment. So, it is beneficial to have the means to either transmit or receive information from their surroundings to act accordingly.

Cellular communication (or cell signaling) is how the cell receives and transmits information to the environment. It is a fundamental ability of all living cells and allows for complex cooperation, whether bacterial or eukaryotic cells. For instance, when they reach a certain number of individuals, several strains of bacteria possess the ability to start behaving cooperatively. This type of cooperation is known as quorum sensing; this information reaches the individual cells, who upregulate specific genes when the population reaches a threshold.[1] An example of this phenomenon is the light that the symbiotic bacteria species *Vibrio fischeri* emits by an increasing the synthesis of the protein luciferase when induced by its host. This symbiosis allows the host to take advantage of the bacterias' bioluminescence, for instance, utilizing the light during nocturnal activities.[2]

Cells can react to many stimuli, either physical (pressure, electricity, light, or temperature) or chemical (small molecule, protein/peptide interactions). The common denominator in receiving information from the surroundings is cellular receptors present in the cellular membrane.[†] Upon activation, the receptor undergoes a conformational change that starts a cascade of molecular events via second messengers, which ultimately corresponds to a cellular response (Figure 1.1). The cellular response can vary from gene regulation to metabolic adjustments. This pathway is known as signal transduction and allows the organism to transport the molecular message from the receptor (located in the membrane) to the relevant part of the cell.

[†] They are also present in the nuclear membrane and organelle membranes

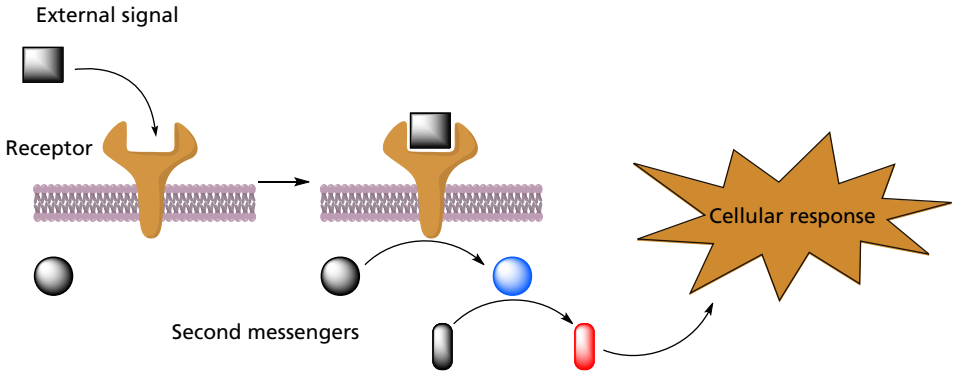

Figure 1.1: A general, simplified overview of signal transduction.

Cells are complex biological entities with multiple interactions with their surroundings. Therefore, a suitable information carrier needs to be able to handle this complexity. Cells might need additional assistance and recognition to facilitate interactions between the target receptor and the signaling molecule. To illustrate, they could use proteins, but there is a limit to the information presented by peptides. There are around 20 amino acids to utilize, but they can only be connected linearly. For example, a dipeptide of the amino acid serine would only allow for one combination. However, a disaccharide of the carbohydrate glucose would allow for significantly more combinations, that is, 11 different connections (Figure 1.2). This higher number is due to multiple hydroxyls present and possible anomeric linkages (see Section 1.4 for more details on carbohydrate structure).

Since this is just the connectivity of one type of carbohydrate, the potential versatility of carbohydrate-based signaling is astonishing. If factoring in all possible D-sugars and possible branching, there are $1.05 \cdot 10^{12}$ possible, different hexasaccharides.[3] This is in comparison to peptides or nucleotides, which have $20^6 = 64'000'000$ and $4^6 = 4096$ combinations, respectively. Worth noting is that glycosylations of proteins can also mediate critical features such as stability, localization, and ligand specificity.[4] Not very surprisingly, the cell surface is filled with glycoproteins that act as binding partners for a considerable variety of biomolecules. The cell's carbohydrate layer is known as the glycocalyx; it can reach a thickness of several hundred nanometers and even hide membrane-bound proteins.[5]

Since carbohydrates mediate cellular communication, they are also involved in disease progression. There are multiple ways this can occur, but commonly it is not the carbohydrates themselves that are agents of illness. Instead, they are tools that other agents utilize. As an example, cancer cells change their glycosylation patterns to mediate metastasis and growth.[6] This involves changes in branching, truncation, and increasing amounts of particular monosaccharides.[7] Another example is the ability of

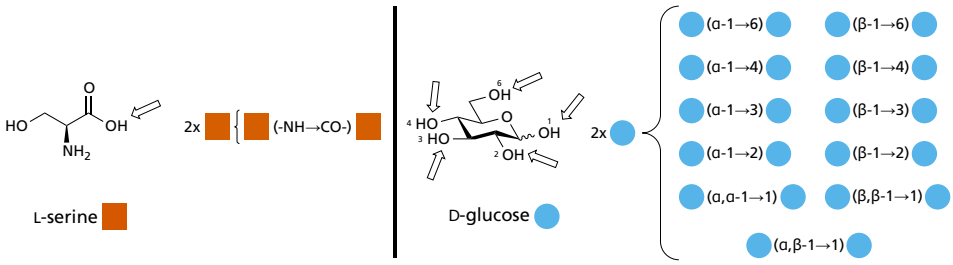

Figure 1.2: A comparison of the difference in potential connectivity between an amino acid and a monosaccharide (Section 1.4 elaborates on carbohydrate nomenclature α and β).

the immune system to recognize foreign organisms via carbohydrate-recognizing proteins known as lectins.[8] However, if the bacteria can alter their expression of glycans, they can avoid the immune system and cause infection.[9] So, to find new therapeutics, we need to understand the different components of the glycocalyx, how the cells create them, and how they interact with other biomolecules.

1.2 Proteoglycans/glycosaminoglycans

There are two major classes of carbohydrate-containing molecules in the glycocalyx: glycoproteins and glycolipids. The common denominator is that carbohydrates are covalently attached; to proteins for glycoproteins and to lipids for glycolipids. These carbohydrates are collectively known as glycans. Glycoproteins and glycolipids have essential functions,[10,11] but this thesis focuses on the glycoprotein subclass proteoglycans (PGs),[12] and their role in cell signaling. Figure 1.3 depicts these classes of biomolecules.

PGs consist of a core protein scaffold that extends into the extracellular matrix (ECM) with one or several long, anionic, carbohydrate chains covalently attached. There are two distinguishing features of PGs. The first is the branching; other glycoproteins have branched glycans while PGs have linear glycans. The second is the carbohydrate content; other glycoproteins usually contain around 15% carbohydrates by mass. That number for PGs is about 50%.

The glycans in PGs are known as glycosaminoglycans (GAGs). They were discovered in the middle of the 19th century when GAG chains were isolated from cartilage tissue.[13] Virtually all cell types express PGs, with the distinction being the expression of different families.[14] The GAGs are responsible for the interactions with other biomolecules.

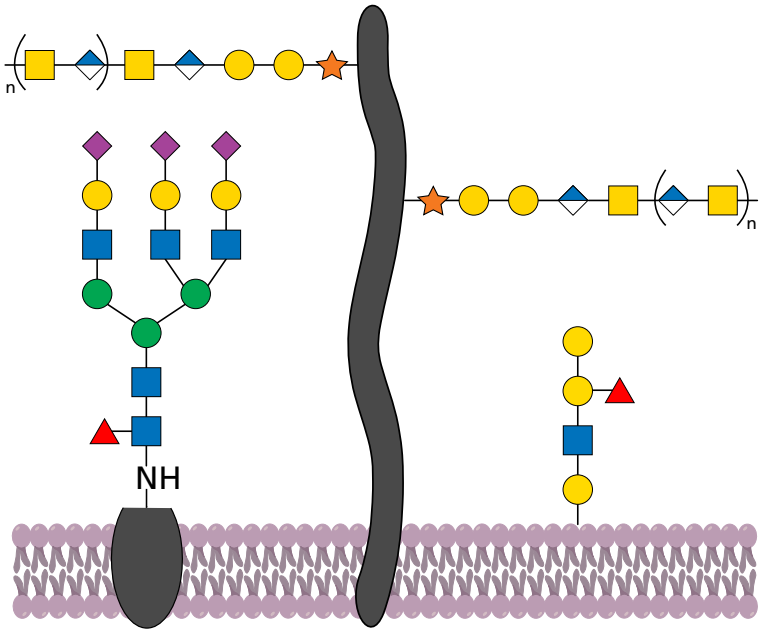

Figure 1.3: The general structures of carbohydrate-containing molecules in the cellular membrane: From left to right: glycoproteins, the glycoprotein subclass proteoglycans (the focus of this thesis), and glycolipids. Shapes correspond to different types of carbohydrates.

Proteins that interact with GAGs are amyloidal proteins (matrix interactions), thrombin/antithrombin (coagulation cascade), ApolipoproteinA-V (lipid interactions), cytokines/TNF-α (inflammation), and hedgehogs[†]/TGF-β (growth factors) for example.[14]

There are four families of GAG structures: Heparin/Heparan sulfate (HS), Keratan sulfate (KS), Dermatan/Chondroitin Sulfate (CS/DS), and Hyaluronic Acid (HA), and their general structures are depicted in Figure 1.4. Besides HA, the only soluble GAG, they comprise a linker region followed by alternating disaccharides. For KS, this linker region is branched; however, the rest of the GAG is linear.

These disaccharides are characteristic of the GAG family. They are composed of a hexosamine (N-acetyl-D-galactosamine (D-GalNAc)- or N-acetyl-D-glucosamine (D-GlcNAc)) and a uronic acid[‡] (D-glucuronic acid (D-GlcA) or L-iduronic acid (L-IdoA)). As the cell synthesizes the polymer, it modifies it by epimerization (i.e., converting GlcA to IdoA) and sulfation (i.e., adding one or more sulfate groups to the carbohydrate). Deacetylation precedes sulfation of an amino group (i.e., removal of

[†] Unfortunately, these are not REAL hedgehog animals, even though it would be somewhat hilarious to imagine.

[‡] For KS, this is a hexose: galactose.

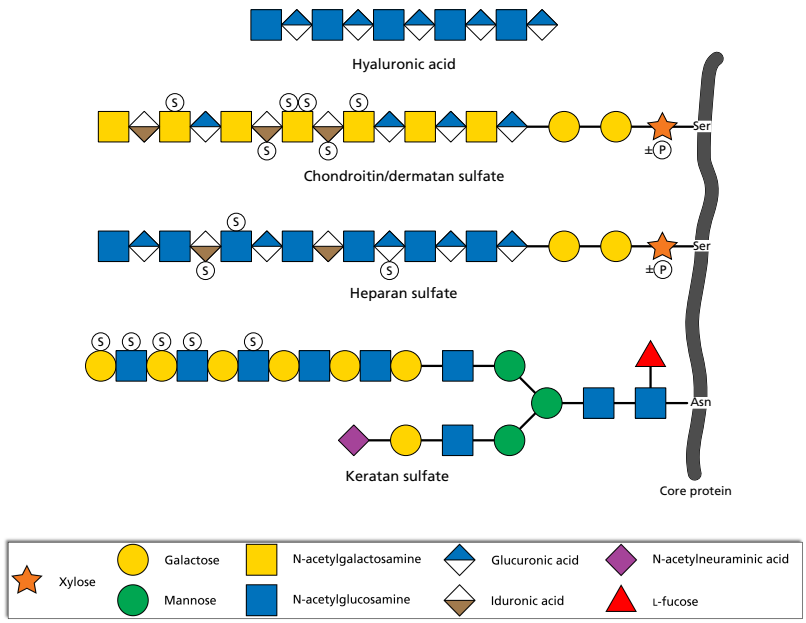

Figure 1.4: A general representation of the different GAG families. Carbohydrates with longer bonds depict linker regions. S=sulfation, P=phosphorylation.

the N-acetyl group in GlcNAc).

Biosynthesis of PGs takes place in two central compartments in the cell (apart from the synthesis of HA, which occurs at the plasma membrane)[15]: the endoplasmic reticulum (ER) and the Golgi apparatus. For the most studied GAGs, that is, HS and CS/DS, xylosylation of one or more specific repeats in the core protein catalyzed by XYLT1 initiates the synthesis. Next follows two galactosylations, performed by β4GalT7 and β3GalT6. Next, GlcAT-I adds a GlcA, which completes the linker region of HS and CS/DS GAG families. The synthesis then diverges; for HS-type, GlcNAcT-1 adds a GlcNAc, and for CS/DS-type, a GalNAcT-1 adds a GalNAc. A summary of the biosynthesis is seen in Figure 1.5.

There is a tremendous complexity in GAGs due to their sheer size and the number of possible post-synthetic modifications.† Compared to regular glycans, which usually contain around 10-12 residues, a GAG polymer can contain around 80.[14] These residues are sulfated or epimerized depending on cell type and, assumably, the different requirements the cell has in the particular moment. GAGs are continuously shed from the cell surface or taken up by endocytosis, resulting in a high turnover rate, thus allowing for dynamic signaling. The rate can vary from a couple of hours to several days.[16,17]

† In comparison to protein and DNA/RNA-synthesis, no template exists for GAG-synthesis.

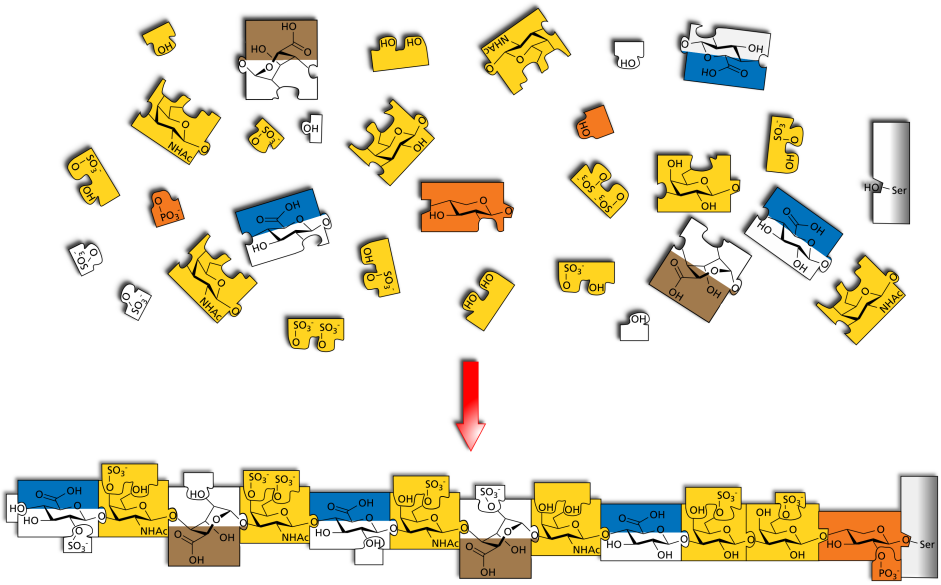

Figure 1.5: Example of the biosynthesis of chondroitin/dermatan sulfate. The cell assembles the polymer with monosaccharide building blocks from right to left, with several enzymes modifying the polymer after elongation.

Also, linker region modifications are observed, such as phosphorylation of *O*-2 in the xylose residue, which seemingly is important for regulation and further synthesis in Golgi.[18,19] Also, possible sulfation of the galactoses can serve as a regulatory function.[20,21]

Several diseases involve mutations in the genes that encode for the proteins involved in GAG synthesis,[14,22] since they are significant for proper cellular communication. For instance, since PGs/GAGs constitute a substantial part of connective tissue/ECM, this can result in Ehlers-Danlos Syndrome (EDS). This collection of disorders is related to an inability to properly process collagen and other structures in the connective tissue. Furthermore, mutations in the enzyme β4GalT7 have been identified as a source of the progeroid variation of EDS.[23–26]

Since the galactosylation of xylose is an early step in biosynthesis, β4GalT7 is a target of great interest for therapeutic intervention.

1.3 β4GalT7

The second enzyme in the GAG biosynthesis is β4GalT7, or β-1,4-Galactosyltransferase 7. It is the seventh member (in order of discovery) of the β-1-4-galactosyltransferase family, and it differs significantly from the other enzymes in the family by not having several conserved cysteine residues.[27] Another key difference is that the enzyme catalyzes the galactosylation of xylose, while the others are involved in galactosylation of Glc or GlcNAc. Thus, β4GalT7 is responsible for the galactosylation of the xylose residue in the linker region.

Almeida and Okajima nearly simultaneously reported cloning and characterization of the enzyme in 1999.[27,28] They identified it as a protein with its N-terminus outside of the membrane (i.e., type II membrane protein) located in the cis-Golgi. Qasba et al. resolved the crystal structure of human β4GalT7 in 2013. This crystal structure revealed that the enzyme operates via an open and closed state similar to other galactosyltransferases, illustrated in Figure 1.6, top.[29] The catalytic cycle is represented in Figure 1.6, bottom.

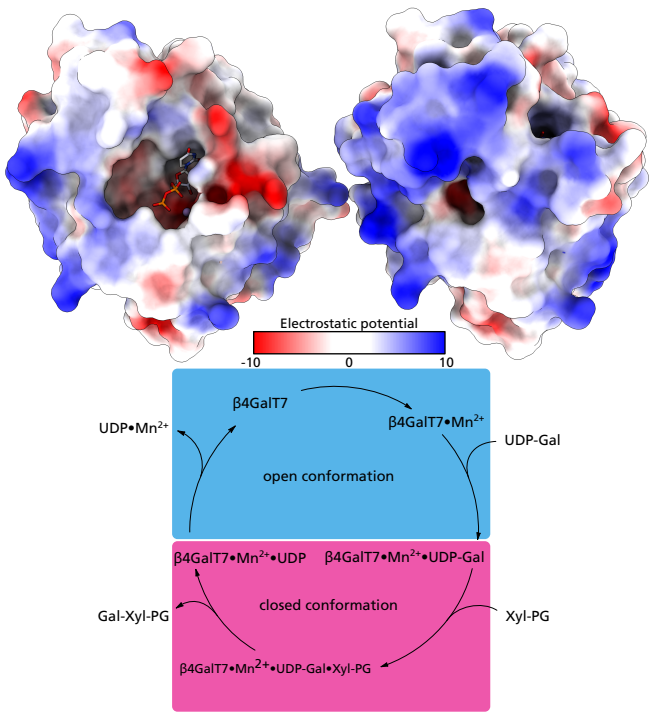

Figure 1.6: Top: Human β4GalT7 in the open conformation (left, PDB 4IRQ), and closed conformation (right, PDB 4IRP) in complexation with UDP and Mn^{2+}. The xylose binding pocket with the surrounding hydrophobic amino acids forms upon conformational change. **Bottom**: The catalytic cycle of β4GalT7.

In general, enzymes catalyze reactions by lowering the energy for the reaction's transition state, that is, by interacting in a specific manner with the substrate with precisely placed side chains. These interactions make the reaction very specific and highly efficient. However, a key feature of catalysis is that only the kinetics of the reaction is affected, not the thermodynamic equilibrium. This observation, together with the fact that it is possible to observe a maximum velocity,[†] implies that the activated complex exists at a definite concentration, where all active sites are saturated.

These facts allowed Leonor Michaelis and Maud Menten to propose a model for enzyme kinetics (Equation (1.1).[30,31] Based on this model, it is possible to make a simplified equation describing the velocity. This simplification is possible by assuming a steady-state reaction while also assuming that the substrate is present in a much higher concentration than the enzyme. This equation is known as the Michaelis-Menten equation (Equation 1.2).

$$\mathrm{E} + \mathrm{S} \underset{k_{-1}}{\overset{k_1}{\rightleftharpoons}} \mathrm{ES} \xrightarrow{k_2} \mathrm{E} + \mathrm{P} \tag{1.1}$$

$$V = V_{max} \frac{[S]}{[S] + K_m} \tag{1.2}$$

K_m is the Michaelis constant, and it is defined as follows (Equation 1.3). k_{cat}, or technically k_2, is the rate-determining step.[‡] k_{cat} is also known as the turnover number, that is, the rate that the enzyme converts substrates to products.

$$K_m = \frac{k_{-1} + k_{cat}}{k_1} \tag{1.3}$$

The features of Michaelis-Menten enzyme kinetics is illustrated in Figure 1.7. Two key parameters for enzyme kinetics, K_m and k_{cat}, can be extracted from this plot. K_m is defined as the concentration where $V = \frac{V_{max}}{2}$. We acquire k_{cat} by Equation 1.4, and we obtain the value for V_{max} when the substrate concentration is much greater than the enzyme concentration so that the velocity reaches a plateau.

$$k_{cat} = \frac{V_{max}}{[E]_{total}} \tag{1.4}$$

[†] Several enzymes, however, have such high catalytic efficiency that the rate-limiting step of the reaction is the diffusion of substrate into the enzyme (which is the theoretical limit of catalysis efficiency).

[‡] Since it is the kinetically important step, possible consecutive steps are usually omitted.

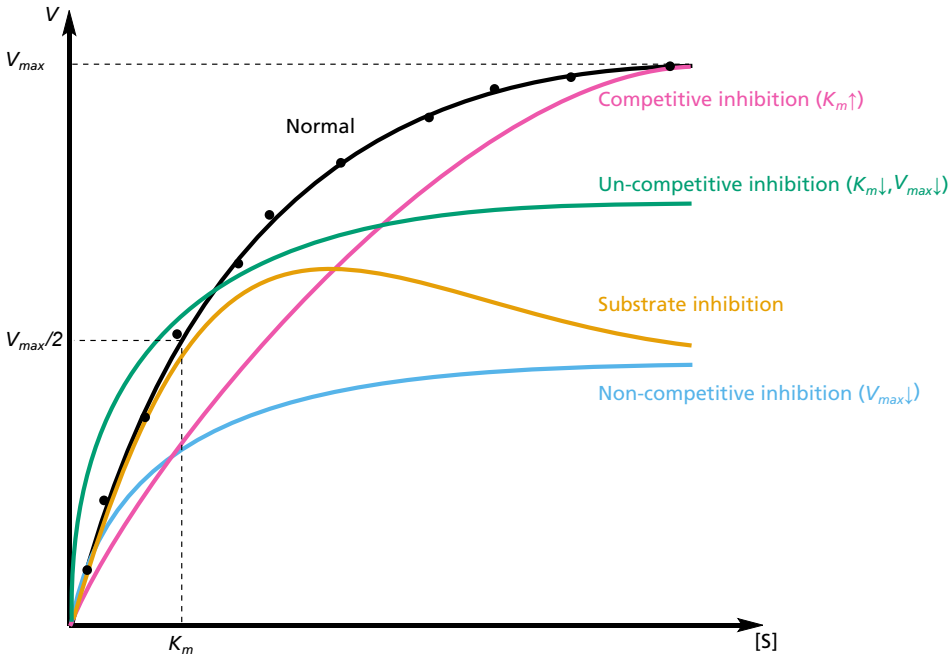

Figure 1.7: Michaelis-Menten kinetics, and how it is affected by different modes of reversible inhibition. [E] is the same in all cases.

To put the different parameters in context, we can use K_m and k_{cat} to compare different substrates and inhibitors. K_m is the concentration where we observe significant catalysis, dependent on the substrate and conditions (pH, temperature, ionic strength). It also indicates how easily the enzyme-substrate complex forms and how strong the enzyme interacts with the substrate. Therefore, to compare enzymatic activity on different substrates, a good option is to compare the catalytic efficiency, that is, k_{cat}/K_m, since this considers both enzyme-substrate interactions and the rate of catalysis.

Substrates can also inhibit the enzyme in different ways (Figure 1.7). If the inhibitor binds to the active site but no product forms, the principal reaction will be slower (i.e., a competitive inhibitor). V_{max} will still be attainable, but K_m will increase as we need higher concentrations to observe significant catalysis. Similarly, if the inhibitor only binds to the enzyme-substrate complex (i.e., an un-competitive inhibitor), this will decrease K_m via Le Chatelier's principle.[†] V_{max} will also decrease due to the inability to complete the catalysis.

[†] Since there will always be unproductive inhibitor-enzyme-substrate complex present, this pushes the equilibrium towards the enzyme-substrate complex, reducing K_m.

If the inhibitor binds allosterically to another site than the active site (i.e., a non-competitive inhibitor), this will not interfere with substrate binding to the active site. However, this slows catalysis due to altered conformation of the enzyme, so V_{max} decreases, but K_m remains the same. When an increased amount of product reduces velocity, this is known as substrate inhibition.[32,33] This has been observed with cloned β4GalT7.[34,35] It is worth noting that the substrate concentration *in vivo* is typically less than commonly used in enzymatic assays.

To evaluate whether a molecule acts as a substrate or inhibitor of β4GalT7, we must assess this by some means. Enzymatic activity of β4GalT7 has been evaluated in several ways: by absorbance or fluorescence,[18,35–37] radioactive labeling,[27,38] or NADH coupling.[35]

Briefly, we used human β4GalT7 expressed as a polyhistidine-tagged glutathione S-transferase fusion protein to facilitate purification for the assay employed in this thesis.[39,40] The enzyme was incubated with the xyloside of interest with UDP-Gal and Mn^{2+} under conditions optimized to give a first-order dependence on the product formation. The reaction progress was analyzed by high-performance liquid chromatography (HPLC) using fluorescence detection, plotting the increase of product with an increasing amount of substrate. Inhibition was analyzed by comparing the integrals of the product with or without inhibitor present.

The importance of investigating how different structural features of the substrate alter the enzyme's activity is central to enable the design of molecules that could function as either substrates or inhibitors. If a structural element seems to improve the activity, this can guide the design of new, more efficient substrates. In the same way, if a feature seems to diminish activity, this guides the design of enzymatic inhibitors. This approach could enable therapeutics of diseases by modulating the activity of the enzyme. In the case of β4GalT7, efficient primers or inhibitors would directly affect the biosynthesis of GAGs.

1.4 Xylosides

As mentioned previously, carbohydrates are a family of chiral[†] biomolecules that consist of a polyhydroxylated carbon chain containing a carbonyl functionality.

The carbohydrate nomenclature is summarized in Figure 1.8. If the carbonyl is an aldehyde, the carbohydrate is considered an aldose; if it is a ketone, it is called a ketose.

[†] Chiral refers to a property of asymmetry, that they can exist in either a "righthanded" or "lefthanded" form that cannot be superimposed. This is a very important feature in biomolecules.

The most abundant carbohydrates in nature, such as glucose and galactose, contain six carbons and are thus labeled as hexoses. If one carbohydrate unit does not form subunits while subjected to hydrolysis by aqueous acid, it is called a monosaccharide.

The Fischer projection, a linear projection with the carbonyl at the top, with a vertical line representing the carbon chain, is a common way to depict the configuration of the carbohydrate stereocenters. The specific relation of the stereocenters in the Fischer projection decides the name of the carbohydrate. In contrast, the absolute orientation of the hydroxyl furthest away from the carbonyl decides whether it is a D or an L carbohydrate (Figure 1.8).

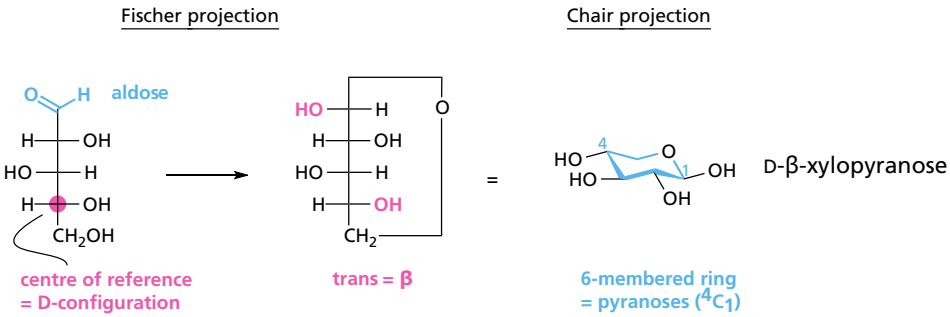

Figure 1.8: Carbohydrate nomenclature concepts (illustrated with β-D-xylose). $^4C_1$ signifies that carbons 4 and 1 are above and below the plane of the ring, respectively.

We mostly find carbohydrates in a cyclic form in nature, but we can also observe minute (sometimes negligible) amounts of the linear form. The cyclic form occurs when hydroxyls on the chain react with the carbonyl to form a hemiacetal. We usually depict this form as a chair form (though several other conformations are available) with a descriptor signifying the type of spatial arrangement.

For example, a six-membered ring is called a pyranose form, and a five-membered ring is called a furanose form (other ring sizes exist but are rare). We call the newly formed chiral center the anomeric carbon, and it is designated α or β depending on its relationship with the specified reference stereocenter in the carbohydrate. For example, if they are cis in the Fischer projection, they are designated α; if they are trans, β.

Xylose is a carbohydrate that consists of a five-carbon chain, have an aldehyde as the carbonyl functionality, and does not form subunits by treatment with aqueous acid. Therefore, it is an aldopentose monosaccharide. We refer to a xylose connected to another molecule as a xyloside. Moreover, we refer to the group that is bound to the anomeric carbon on xylose as the aglycon.

Xylose exists mainly as a significant component in hemicellulose, from which it was also first isolated (xylose is also known as "wood sugar," from the Greek word $\xi\psi\lambda o\nu$, *Xylon* meaning "wood"). However, in mammals, xylose is almost solely found in the linker region of GAGs, as previously mentioned.

We often use conventional carbohydrate chemistry to synthesize xylosides, that is, activating a xyloside donor with an activator (commonly a Lewis acid). At this point, an acceptor group reacts with the formed oxocarbenium ion (Figure 1.9, a). Commonly, this is an alcohol, but other heteroatoms such as sulfur or nitrogen can also act as acceptors. The ratio of the two anomeric configurations will depend on steric effects, solvent effects, and stereoelectronic effects. In addition, the choice of protecting groups can influence the ratio.

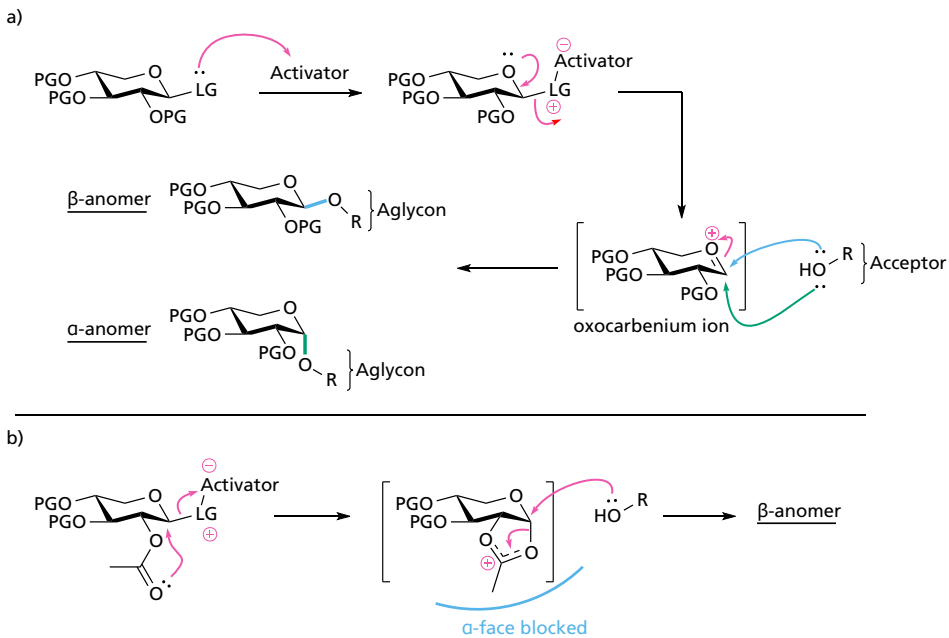

Figure 1.9: a) A general xylosylation reaction. b) Possible neighboring group participation leading to the β-anomer. PG = Protecting group, Activator = Brønstedt- or Lewis-acid.

A carbonyl-containing group at C-2 favors the β-anomer due to neighboring group participation, where a transient intramolecular cyclization shields the bottom face (Figure 1.9 b). Depending on the donor, the mechanistic pathway can proceed either via the described S_N1-type mechanism or an S_N2 mechanism, where the acceptor directly displaces the leaving group.

It is possible to use exogenously supplied xylosides to initiate GAG biosynthesis. Using enzyme isolated from chick cartilage, Helting and Rodén were able to galactosylate free xylose in vitro in 1969.[41] Similarly, Fukuyama showed in 1973 that *p*-nitrophenol-β-D-xyloside functioned as a substrate, and a few years later that it was possible to initiate CS biosynthesis in chicken cartilage, and that it was greatly affected by the structure of the aglycon.[42]

In this thesis, the two primarily used xyloside scaffolds are 2-naphthyl-β-D-xylopyranoside **1**, and 2-(6-hydroxynaphthyl)-β-D-pyranoside **2**, seen in Figure 1.10.

1 **2**

Figure 1.10: Xyloside scaffolds **1** and **2** used in this thesis.

Briefly, we and others have explored xylosides with variations in aglycon size,[43–50] aglycon-carbohydrate distance,[43,49,51,52] anomeric configuration,[52–57] and single modifications in the xylose moiety (e.g., epimers, amines, deoxy analogs, ethers, ketones, halogens).[39,58–63] A summary of different xyloside modifications can be found in Figure 1.11.

In brief, many xylosides function as primers, and the structure of the primed GAGs seems to depend on the features present in the xyloside. Minor structural modifications seemingly influence which type of GAG the cells prime as well as modifications such as epimerization and sulfation. β4GalT7 tolerates very few xylosides modified in the carbohydrate moiety. However, inhibition can also be achieved with some xylosides, notably xylosides substituted in position 4 by fluorine.[52,62] Some naphthosylosides have also been shown to act as inhibitors.[39,60]

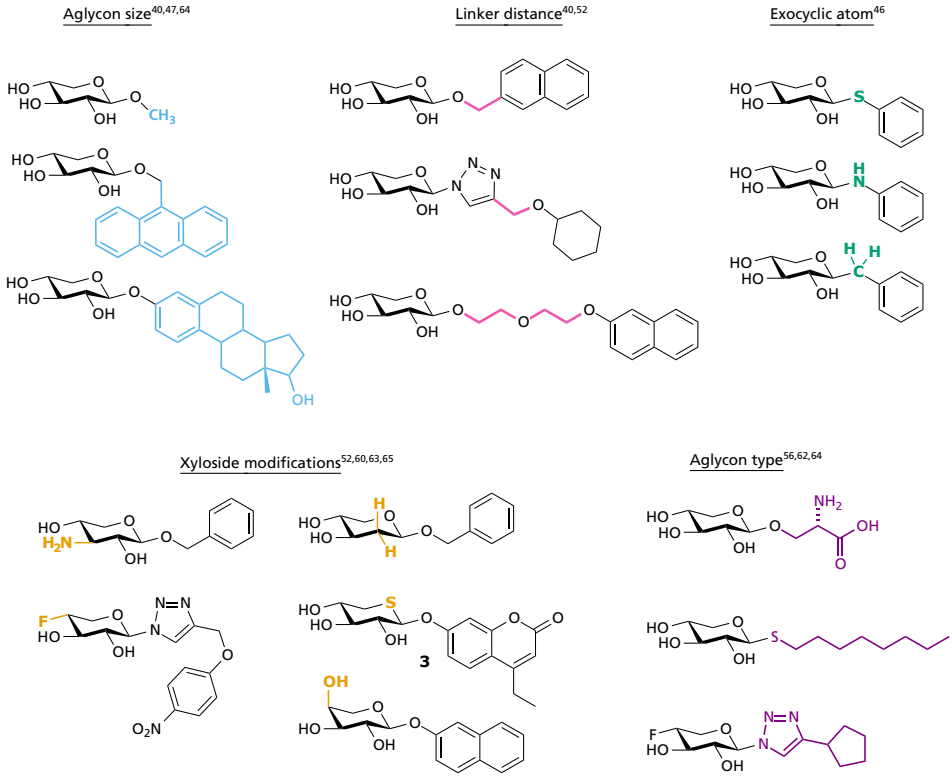

Figure 1.11: A range of different synthesized xylosides and their respective investigative feature.

However, changing the endocyclic atom may improve priming ability. For example, Bellamy et al. discovered that changing the endocyclic oxygen for sulfur resulted in compounds that could function as antithrombotics (compound **3** in Figure 1.11).[64] At the time of writing, these compounds had reached phase II clinical trials, with promising results.[65–68]

Since xylose is such an uncommon carbohydrate in mammals, and in conjunction with β4GalT7 being involved so early in GAG biosynthesis, xylosides are exciting targets for clinical intervention by either increasing the priming of soluble GAG-chains or inhibition of the biosynthesis. However, to use xylosides in a clinical setting, we need tools to investigate the parameters controlling GAG synthesis and GAG interactions with biomolecules of interest.

1.5 Introductory key points

The key points from Chapter 1 are:

- Carbohydrate-protein interactions largely influence cellular signaling.
- PGs and GAGs are significant contributors to these interactions by being large, highly charged molecules with great structural variety.
- Biosynthesis of GAGs is dependent on the correct synthesis of the linker region, which presents a pharmacological target of great interest in β4GalT7.
- Xylose, the substrate for β4GalT7, is an uncommon aldopentose in animal cells. It is an interesting target for priming or inhibiting the GAG biosynthesis due to its scarcity in mammalian biochemistry.
- Finding ways to modify xylosides would be very useful to discover new primers or inhibitors of β4GalT7. We could then use these molecules to prime or inhibit GAG biosynthesis and learn valuable information regarding potential pharmaceutical targets.

Chapter 2

Thesis objectives

Hopefully, the difficulty of obtaining information from such a complex system as the GAG biosynthesis, is evident from the introduction. Nevertheless, we cannot overstate the importance of the information that carbohydrates carry regarding cellular function.

Therefore, it is of great importance to gather knowledge and facilitate the research of this complex system, especially regarding possible findings of medical importance. As of now, despite the efforts and advancements of fellow scientists, the field of glycobiology is not as well understood as the fields of the other classes of biomacromolecules (e.g., proteins and DNA).[69]

In this project, we posed several hypotheses regarding xylosides and GAG biochemistry:

- Altering the endo/exocyclic heteroatom in xylose will influence the priming kinetics in β4GalT7.
- Substituting multiple hydroxyls in xylose provides inhibitors of β4GalT7.
- It is possible to make an efficient inhibitor of β4GalT7 by combining a UDP fragment with a naphthoxyloside fragment.
- Functionalizing the aglycon of the xyloside will enable the investigation of biosynthetically relevant GAG-related questions.
  - A deuterated naphthyl simplifies mass spectrometry analysis by clear differentiation of fragment mass.
  - A fluorophore aglycon allows visualization of GAG-movement in cells using confocal microscopy.
  - An amine/azide attachment allows functionalization of cell primed GAGs and subsequent analysis by biophysical techniques.

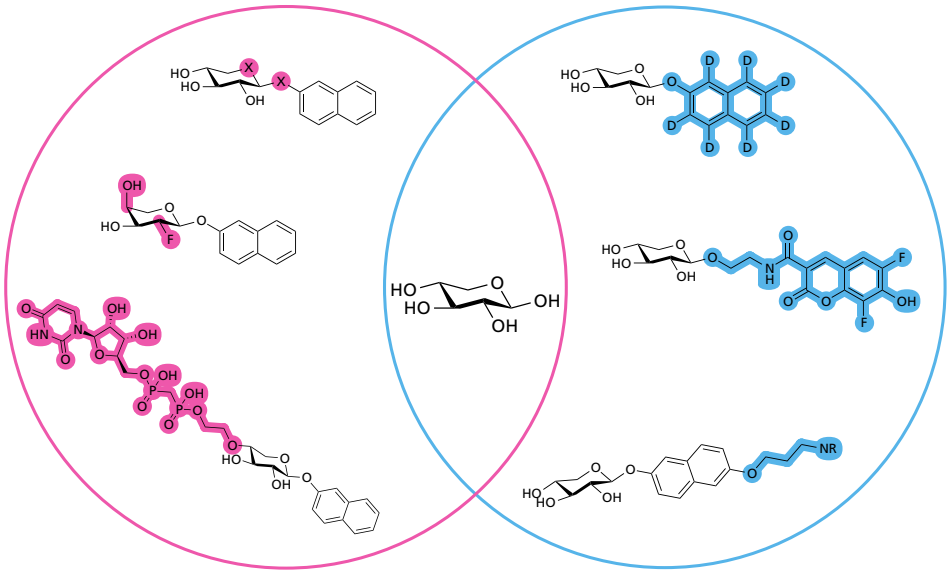

Figure 2.1: Main thesis objectives represented in a Venn-diagram with the common denominator in the middle. **Red**: modifications of xylose moiety for priming/inhibition studies in β4GalT7. **Blue**: aglycon modification for investigations of GAG biosynthesis in cellular culture.

By synthesizing different xylosides, these hypotheses could be answered and make progress towards the understanding of GAGs and possibly uncover new possibilities for selective pharmacological targets. By modifying the xylose moiety, it should be possible to probe the key constraints for priming or inhibition of GAG synthesis. On the other side of the carbohydrate scaffold, modifications of the aglycon (without disrupting priming ability) could give new properties to the xylosides and allow us to probe aspects of the cellular processes that govern GAG biosynthesis and function. Those are the main aspects that the work of this thesis has focused on (Figure 2.1).

Chapter 3

Xyloside Modifications

3.1 Endo- and exocyclic oxygen substitutions (Paper I)

Due to the different sizes and bond angles of heteroatoms, it is possible to make minor adjustments to the bond angles and the positioning of the aglycon by exchanging one heteroatom for another, for instance, oxygen to sulfur. To investigate such small influences on β4GalT7 the substrate specificity of β4GalT7, we decided to make a set of xylosides with different heteroatoms in the aglycon bridge and the carbohydrate ring (Table 3.1).

Table 3.1: Different naphthoxyloside analogs with endo (red) and exocyclic (blue) heteroatom substitutions of interest in this study.

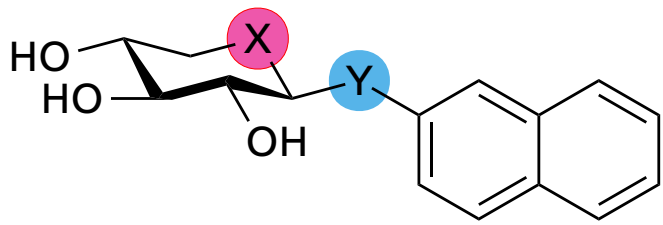

Compound	Endocyclic (X)	Exocyclic (Y)
1	O	O
4	O	S
5	S	O
6	S	S
7	CH_2	O
8 (L-7)	CH_2	O

We decided to include **4** in this study; it had already been synthesized but not evaluated in a β4GalT7 assay.[43] Also, there was a conflict in the literature; the L-enantiomer of **3**, namely **9**, which is structurally similar to **7**, could presumably act as a substrate,[67] which is in disagreement with other investigations.[67,70,71] Therefore, it was of great interest to see if the L-enantiomer of **7**, that is **8**, could serve as a substrate or not (Figure 3.1).

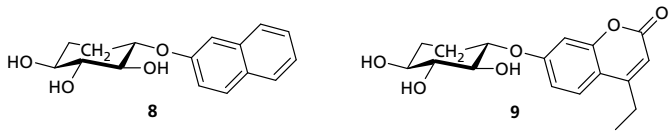

Figure 3.1: Structures of our target **8** and compound **9**, reported to act as a substrate for β4GalT7.

3.1.1 Synthesis

Scheme 3.1 shows the synthesis of the new targets. We used a convergent synthetic strategy to reach the carbocyclic analog and its L-enantiomer; we utilized chemistry developed by Madsen et al.[72,73] and Kornienko et al.[74,75] for the D-xylo and L-xylo configurations, respectively.

Starting from **10** for the L-configuration, a Wittig olefination of the acyclic form of **10** gave **11**, which after oxidation provided aldehyde **12**. The material for D-configuration began from iodinated glucose derivative **13**, which was reductively fragmented to give **14**. Interestingly, the choice of solvent and a chelating salt allows more stereocontrol in the Grignard addition making **15** and **16**.[74] Therefore, changing the solvent of the reagent from THF to CH_2Cl_2, and adding $MgBr_2$ improved the selectivity for the *anti*-addition.

A ring-closing metathesis gave **17** and **18**, and a Mitsunobu reaction installed the naphthyl aglycon to give **20** and **19**. Removal of protecting groups while simultaneously reducing the olefin gave the two enantiomers **7** and **8**.

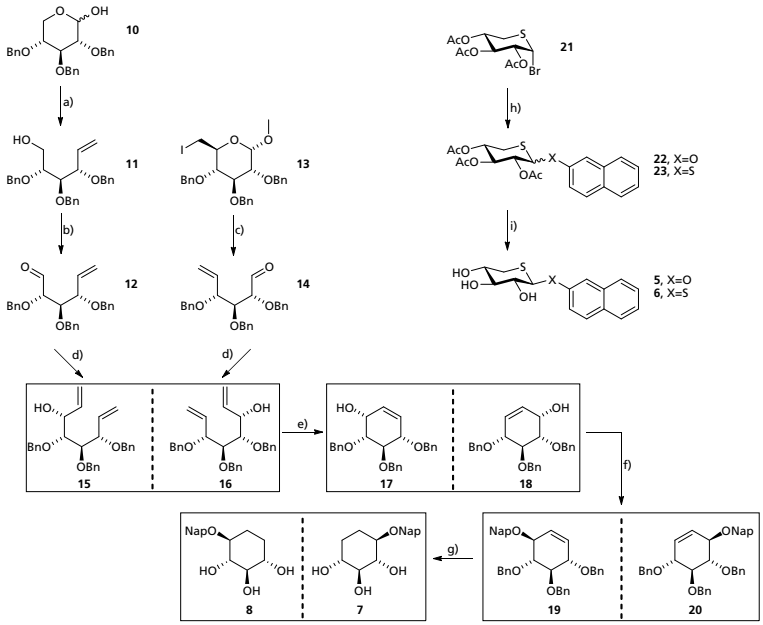

Scheme 3.1: Synthesis of the different targets. Reagents and conditions: a) Ph_3PCH_3Br, BuLi, THF, **11** (65%); b) $COCl_2$, DMSO, Et_3N, CH_2Cl_2, -78 °C; c) Zn, THF/H_2O, ultrasound, d) EtMgBr, $MgBr_2$, CH_2Cl_2, -78 °C, **15** (79% over two steps), **16** (50% over two steps); e) Grubbs catalyst (1st gen), CH_2Cl_2, **17** (91%), **18** (%); f) 2-naphthol, DIAD, THF, **19** (24%), **20** (51%); g) HCl (conc. 22 eq), Pd/C (10 mol%), H_2 (1 atm), DMF, **7** (31%), **8** (50%); h) 2-naphthol or 2-naphthalene-thiol, ZnO-$ZnCl_2$, toluene/MeCN (1:1), Δ, **22** (α/β 0.9:1), **23** (54%); i) NaOMe (0.05 M), MeOH, **5** (2% over two steps), **6** (97%).

We synthesized the 5-thio analogs from the known donor **21**.[76] The synthesis of the dithio-analog **6** proceeded well using ZnO-$ZnCl_2$ as a promotor, followed by deacetylation in NaOMe/MeOH to give **23**.[77] **22** was more difficult to reach due to a side reaction that favored the *C*-xyloside. The thermodynamic *O*→*C* rearrangement of aromatic aglycons of *O*-xylosides and *C*-xylosylations with thioxyloside donors is previously known.[78–80] This rearrangement was revealed to be a significant synthetic hurdle. However, it was possible to obtain enough material of **4** to analyze the compound in the β4GalT7 assay. We tested several procedures (i.e., phase-transfer catalysis (PTC), different Lewis acids, S_N2 type reactions) in our attempts to reach **5**, resulting in either the *C*-xyloside **24** or **25** (Figure 3.2).

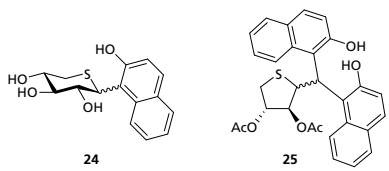

Figure 3.2: The different *C*-xyloside products **24** and **25** obtained in the attempted syntheses of the 5-thio-β-D-xyloside analogs.

3.1.2 β4GalT7 assay

We analyzed the different analogs in the β4GalT7 assay (Figure 3.3, Table 3.2). These findings agreed with previously observed trends with thioxylosides.[64] The L-enantiomer **8** did not act as a substrate in the enzyme assay, despite previous reports.[67] Searching for a solution to this inconsistency, we noticed that the optical rotation of 7 had the same sign as **9**, which the authors assigned as the L-enantiomer. However, since we utilized the chiral pool to synthesize 7 and **8**, we were confident in our stereochemical assignments.

The previously published synthesis of **9** and its D-enantiomer involved an achiral route with the separation of sulfoximide diastereomers.[67] Diastereochemical assignments by NMR can be challenging on xylosides due to conformational flexibility.[81] Therefore, we propose that this discrepancy is due to an erroneous assignment in the literature, and we suggest that L-xylosides are not substrates for β4GalT7.

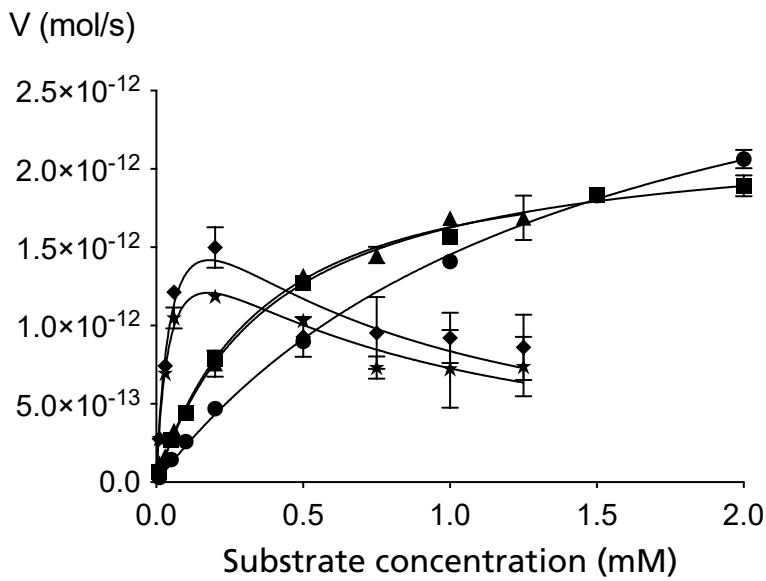

Figure 3.3: Michaelis Menten representation of the activity of β4GalT7 with investigated xylosides **1** (circle), **4** (triangle), **5** (diamond), **6** (star), and **7** (square).

Table 3.2: Kinetic parameters for β4GalT7 galactosylation.

Substance	Structure	K_m (μM)	V_{max} (pmol s^{-1})	k_{cat} (s^{-1})	k_{cat}/K_m ($mM^{-1}\ s^{-1}$)
1	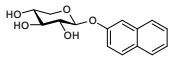	780	2.6	3.1	4.0
4	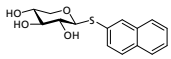	360	2.2	2.7	7.5
5	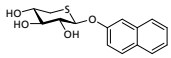	34	1.7	2.0	59
6	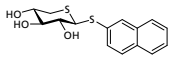	25	1.3	1.6	64
7	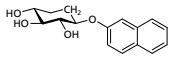	390	2.3	2.7	6.9
8	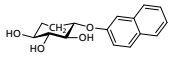	-	-	-	-

The trend observed for the targets as substrates for β4GalT7 was **1**<7<**4**<**5**<**6**. Interestingly, there is significant substrate inhibition of the enzyme observed in the case of the 5-thio- and 1,5-dithioxylosides. As mentioned, the cloned β4GalT7 enzyme is known to exhibit excess-substrate inhibition, but it is unknown if this is true for the wild-type enzyme.[34,35] Therefore, the kinetic parameters have been calculated from the data points before the onset of substrate inhibition (**5** and **6**).

We observed that any modifications, either in the endo- or the exocyclic position, improved priming efficiency. However, the most significant improvement – 15 times – comes from introduction of sulfur at the endocyclic position (**1** vs. **5**). Substitution of the exocyclic oxygen for sulfur improves binding (**1** vs. **4**). Introducing a second sulfur atom to the endocyclic compound does not improve the activity (**5** vs. **6**). Substitution by endocyclic carbon also improves galactosylation (**1** vs. 7), comparable to exocyclic sulfur (**4** vs. 7).

3.1.3 X-ray crystallography and molecular modeling

To investigate this improvement in binding affinity, we decided to make crystal structures of **1** and **6** to see any apparent conformational differences. Upon inspection of the x-ray structure, the sulfur atoms in **6** induced an evident perturbation of the bond angles (Figure 3.4). Thus, smaller bond angles and elongated bonds skew the orientation of the naphthyl moiety.

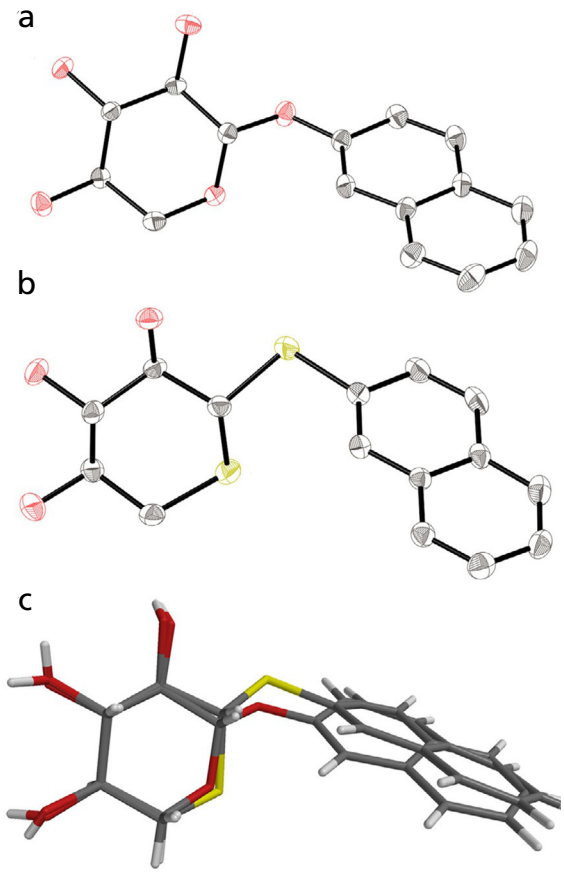

Figure 3.4: Thermal ellipsoid representations of the x-ray structures of a) **1**, b) **6**, and c) superposition. The sulfur atoms induce a distortion of the xylose conformation.

We then probed the active site using molecular docking studies, and **4**, **5**, and **6** fit in the active site of β4GalT7. All the thio analogs display different types of aromatic stacking with the Tyr179 residue, which could explain the improved binding values (Figure 3.5). These interactions are particularly true for **4** and **6**, for which the naphthyl moiety shows aromatic parallel π-stacking, which is a favorable geometry.[82] Also, this reorients the 4-*O* in the xylose moiety, presumably placing it closer to the anomeric carbon of the galactose. For a similar enzyme, β4GalT1, it is proposed that, during deprotonation of 4-*O* in the acceptor, electronic repulsion from the endocyclic oxygen of the donor helps a conformational change to facilitate the reaction.[82] The 4-*O* orientation in analogs **4** and **6** may accelerate this conformational change and improve galactosylation.

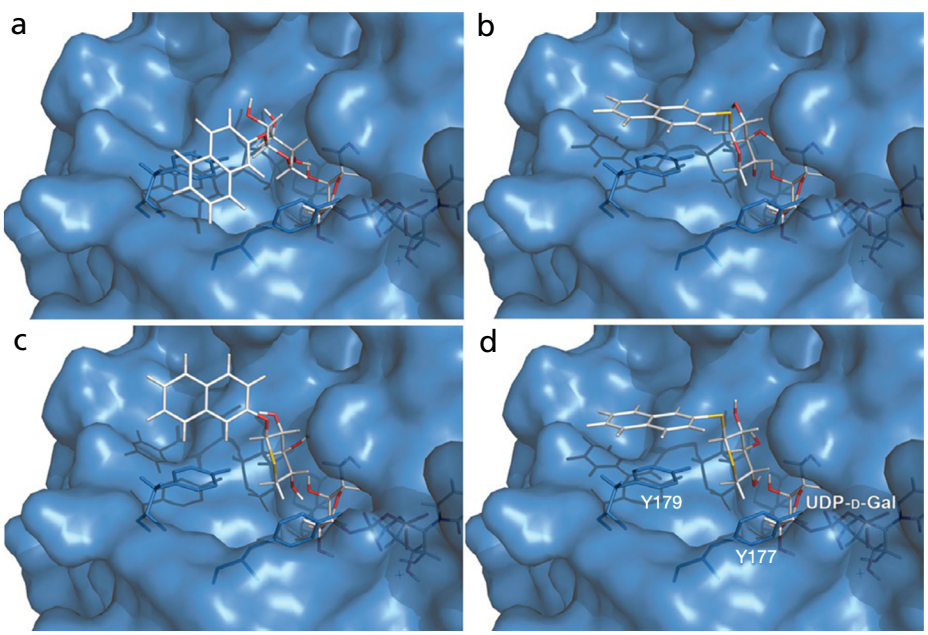

Figure 3.5: Molecular docking of **1**, **4**, **5**, and **6** (a to d respectively). Aromatic parallel displacement π-stacking with Y179 is prominent for **4** and **6**, and T-shaped stacking for **5**.

3.1.4 Conclusions

To investigate how endo- or exocyclic heteroatom substitution affects substrate capability for β4GalT7, we synthesized five different analogs. Due to conflicting reports in the literature, we also investigated if L-xylosides could be substrates for the enzyme. All analogs, except the L-xyloside, acted as substrates in the β4GalT7 assay.

Every modification improved galactosylation from **1**, especially the dithioanalog that was 15 times more efficient. From x-ray crystallography and molecular modeling, we suggest an altered orientation in the active site and aromatic π-stacking as explanations for the increased activity (the parallel displacement π-stacking displayed by sulfur analogs **4** and **6**). From this, we suggest that small changes in orientation influence the priming kinetics in β4GalT7 greatly.

3.1.5 Key findings in Paper I

The key points from Paper I and xylosides with endo/exocyclic modifications are:

- Introducing an aglycon with exocylic oxygen on xylosides is complicated, from a synthetic perspective, due to a $O \rightarrow C$ rearrangement side reaction.
- All modifications resulted in improved substrates for β4GalT7.
- L-xylosides are not substrates for β4GalT7.
- Sulfur modifications significantly alter bond-angles and lengths in xylosides.
- Molecular modeling suggests improved π-stacking of the naphthyl aglycon in the sulfur analogs **4**, **5**, and **6**.
- We could potentially use these molecules to efficiently prime GAG-biosynthesis in cellular systems.

3.2 2,4 di-substitution (Paper II)

Recent investigations, that is, a systematic evaluation of the constraints of the active site of β4GalT7 by modifications of the xylose residue at different positions, revealed the possibility of making naphthyl xylopyranosides that acted as inhibitors (Section 1.4). This made us consider whether multiple modifications could have a synergetic effect and possibly improve the inhibitors. Therefore, we hypothesized that doubly modified analogs are potent inhibitors for β4GalT7. Using the methodology of previous studies,[39,60] we made a 4x4 series of synthetic targets to investigate in our β4GalT7 assay (Table 3.3).

Table 3.3: Different naphthoxyloside analogs with endo (red) and exocyclic (blue) heteroatom substitutions of interest in this study.

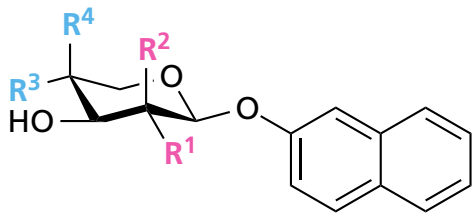

	R^1=OMe	R^1=H	R^1=F	R^2=OH
R^3=OMe	26	27	28	29
R^3=H	30	31	32	33
R^3=F	34	35	36	37
R^4=OH	38	39	40	41

3.2.1 Synthetic considerations

Despite the relative simplicity of xylose, it is complicated to devise a generic synthetic protocol. Many different parameters affect the reactivity of xylose. It is easier to selectively modify the carbohydrate when there is a stereochemical asymmetry, e.g., the presence of axial-equatorial pairs of diols. Compared to the other pentoses, xylose only has equatorial diols, which makes selectivity more challenging.

Regarding the four types of modifications, they all differ in prerequisites and effects (Figure 3.6). Methylation does not induce significant alterations of stereoelectronics. Therefore, this transformation can be considered at any time during synthesis while keeping in mind that there might be reduced selectivity if the remaining hydroxyls are all equatorial. Epimerization significantly alters stereochemical effects and conformational preferences. However, this can introduce a potential for selectivity.

Stereochemical requirements are also important when making deoxyfluorinations since the hydroxyl must have inverted stereochemistry before transformation since the reaction proceeds by nucleophilic substitution via inversion by fluoride. Hence, we must perform the epimerization before fluorination and not vice versa. In addition, deoxygenation removes the functional group and increases instability to acids if performed at 2-OH,[60] which becomes a factor to consider in the subsequent reactions.

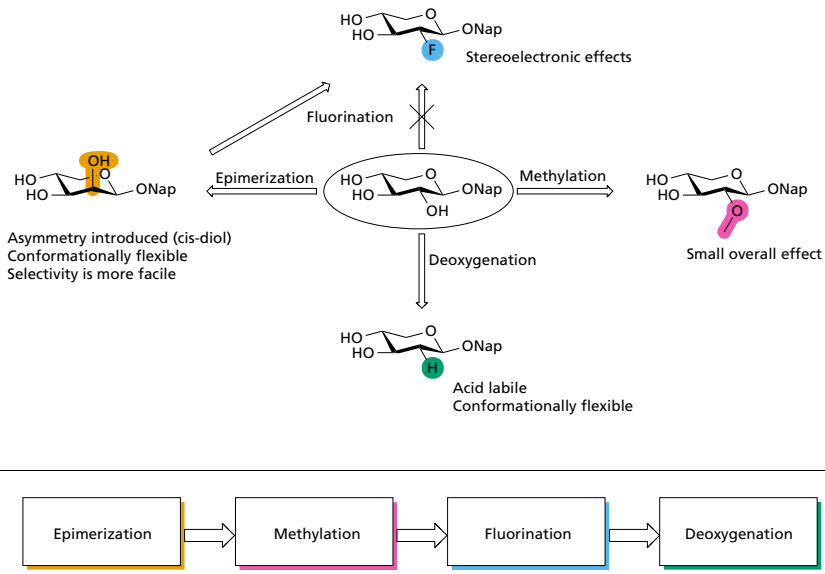

Figure 3.6: General considerations regarding the intended modifications (exemplified at pos 2).

However, while trying to follow the general considerations, the synthesis of these seemingly simple targets proved to be complex. We needed to individually evaluate all the targets due to revelations regarding reactivity or stability of intermediates. Eventually, upon completion, a roadmap for the different targets could be drawn (Figure 3.7).

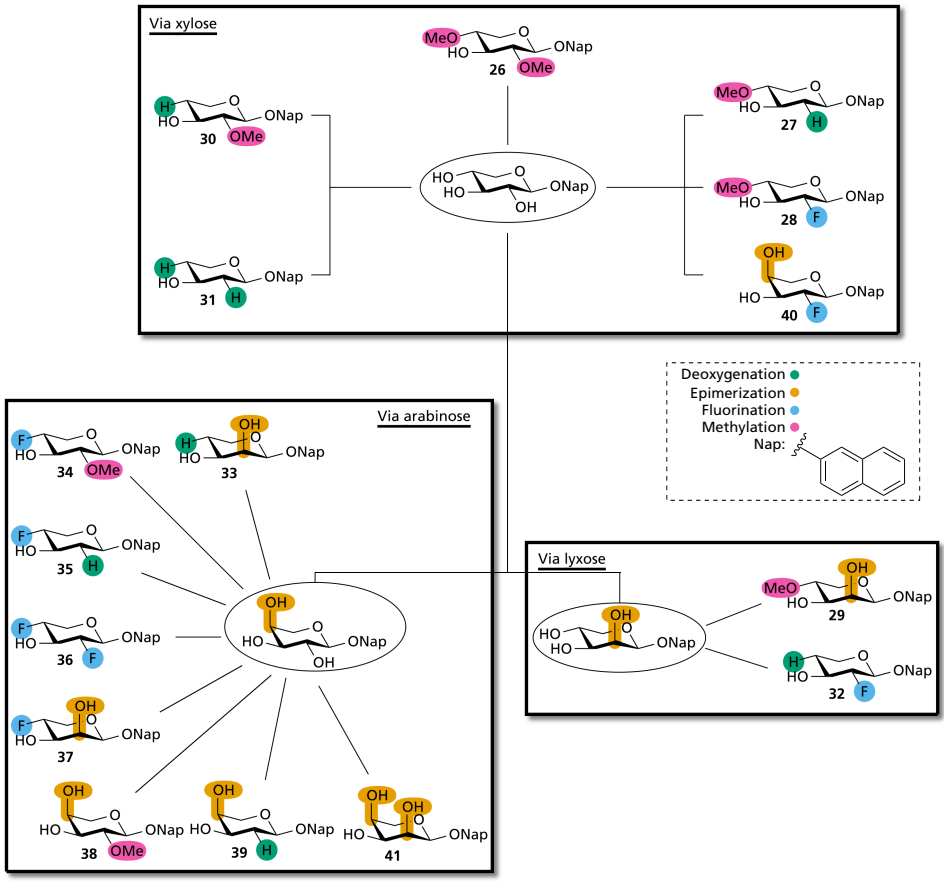

Figure 3.7: Roadmap of the synthetic pathways to the different analogs. Colors are modifications related to the starting xylose molecule.

3.2.2 Synthesis of key pentosides

The synthesis of key pentosides is depicted in Scheme 3.2. We chose **1** as the starting point for synthesizing starting materials since its synthesis is robust.[60] A BDA acetal formation gave **42** and **43** as stable acetals for the free 2-OH and 4-OH, respectively.[60] To reach the arabinose and lyxose configurations, an oxidation-reduction sequence, to utilize inherent ring strain in isopropylidene protected **44** and **46**, was used, followed by deprotection to give arabinoside **45** and lyxoside **47**.[83]

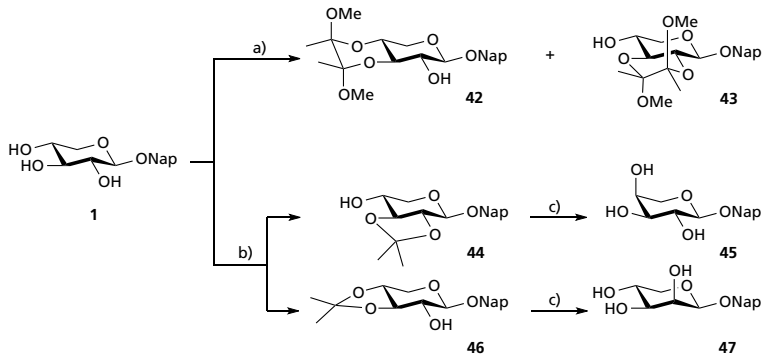

Scheme 3.2: Synthesis of key pentose starting materials. Reagents and conditions: a) 2,2,3,3-TMB, $BF_3 \cdot OEt_2$, MeCN, 3:2 **42**:**43** (quant.); b) 2-methoxypropene, CSA (cat.), DMF, 3 h, 67%, 77:23 **44**:**46** (67%); c) 70% AcOH, **45** (73%), **47** (71%).

3.2.3 Synthesis of targets via xylose

The xylose synthesis pathways are depicted in Scheme 3.3 (the scheme emits mixtures of products for the sake of clarity). The synthesis of intermediates **52**, **57**, and **60** has been published previously but is included here for context.[60]

To reach **26**, we non-selectively methylated **1** and isolated the target via an acetylation-deacetylation sequence from the mixture. Targets **28** and **40** were reached from the common intermediate **52**, obtained via an OTf-based inversion followed by fluorination by DAST from **42**. PTC-methylation of **52** gave target **28** (as a mixture of products), and selective PTC-tosylation gave **53** which then could be inverted and deprotected to give target **40**.

We reached **56** from **42** via a xanthate ester introduction and deprotection, giving **55**, and **56**, respectively. Next, **56** was subjected to a Barton-McCombie deoxygenation to reach **57**. This deoxygenation is a standard method for removing hydroxyl groups,[84] frequently employed with carbohydrates.[85] Due to the increased acid sensitivity of 2-deoxy xylosides, the acetal was removed before the radical reaction.[60] Deoxygenated **57** was methylated to give target **27** among a mixture of products.

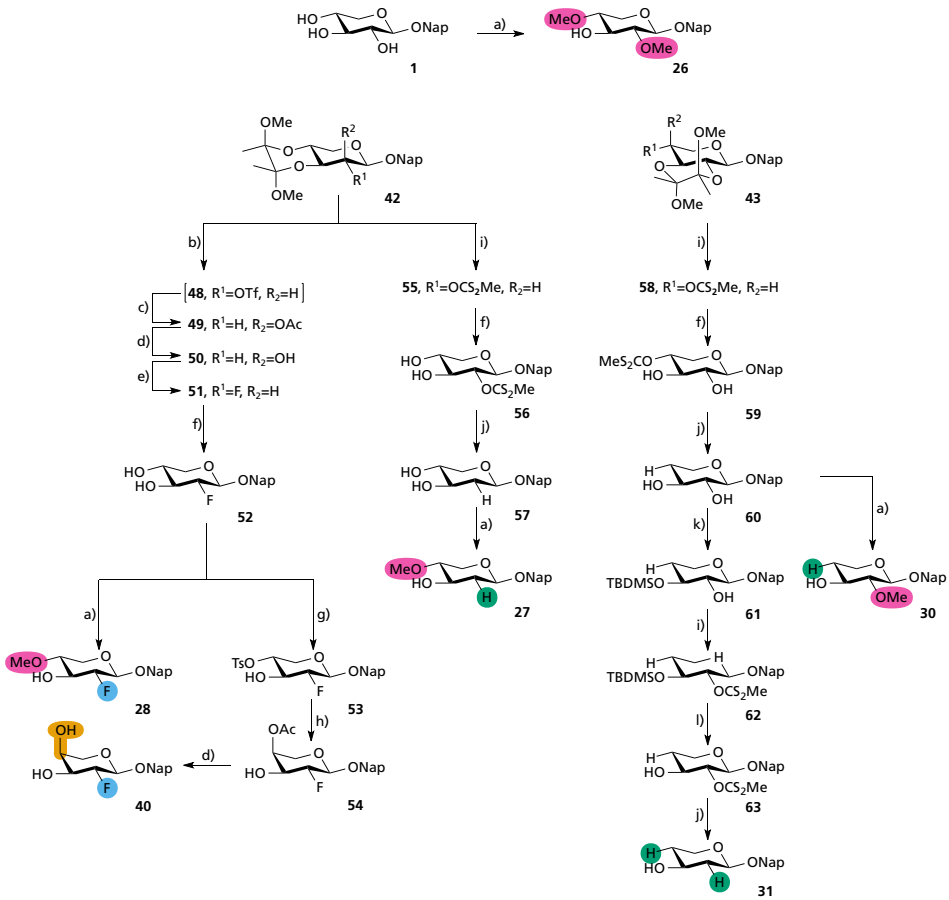

Scheme 3.3: Synthesis of targets via xylose. Reagents and conditions: a) NaH (60% disp. in mineral oil), MeI, DMF 0 °C, **26** (9%), **27** (16%), **30** (42%), or TBAB, MeI, CH_2Cl_2/0.5 M NaOH, **28** (18%); b) Tf_2O, pyr. CH_2Cl_2, -78 °C to 0 °C; c) CsOAc, DMF, 50 °C, **49** (82% over two steps); d) NaOMe (1M), MeOH, **50** (90%), **40** (27% over two steps); e) DAST, CH_2Cl_2, 40 °C, **51** (42%); f) 95%TFA/CH_2Cl_2 1:7, **52** (90%), **59** (62%); g) $TBAHSO_4$, *p*-TsCl, CH_2Cl_2/5% NaOH, **53** (24%); h) AcOH/DBU (12:6 eq), toluene, 90 °C; i) NaH (60% disp. in mineral oil), CS_2, MeI, THF, 0 °C to r.t., **55** (80%), **58** (76%), **62** (83%) j) AIBN (cat.), *n*-$SnBu_3H$ in toluene or H_3PO_2 in 1,4-dioxane, Δ, **57** (30%), **60** (72%), **31** (42%); k) TBDMSCl, DMAP, Et_3N, CH_2Cl_2, MW 100 °C, **61** (48%); l) HCl (1%), EtOH, 0 °C, **63** (85%).

To reach targets **30** and **31**, we used the same approach from intermediate **57**. We began with deoxygenation of 2,3-protected **43** to give **60** as a shared intermediate via **58** and **59**. Interestingly, we observed a skewed selectivity in the methylation of **60** towards the 2-OMe product in a 7:1 ratio. This ratio is in comparison to methylation of **57**, which exhibited an almost 1:1 ratio. Therefore, we needed a way to make a 3-O protected intermediate to proceed towards **31**. We could reverse the selectivity in **60** by using a bulky TBDMS group to mainly form the protected **61**. We finally reached target **31** after deoxygenation and deprotection of **62**, and **63**, respectively.

3.2.4 Synthesis of targets via arabinose

The arabinose pathways are depicted in Scheme 3.4 (the scheme emits mixtures of products for the sake of clarity). Two different protecting group strategies were employed. First, we achieved selective acylation/alkylation of **45** using a borinate catalyst to give the monoprotected intermediates **64** and **65**. These were then fluorinated to give **66** and **67**. However, attempts to epimerize **66** using an oxidation-reduction sequence did not provide the epimer as intended. Instead, we obtained **68** via elimination of the fluorine. We hypothesize that the alkaline conditions and ketone present allow the elimination to proceed via a potential E1cB.

Nonetheless, **68** could be subjected to methanolysis to give target **33**. Furthermore, we could epimerize **67** using an OTf-based approach, using an AcOH/DBU complex as the nucleophilic species to avoid this elimination.[86] **69** was then deprotected to give target **37**. Fluorination of intermediate **70** gave **71**. A modified protocol for hydrogenation provided target **36** since standard protocols saturate the naphthyl aglycon.[87]

For the common intermediate of the remaining targets, **72**, we used an isopropylidene protecting group. Epimerization of **72** and subsequent acetal removal of **73** obtained target **41**. Worth noting is the ring-flip occurring upon reduction of the ketone, even when locked by the cyclic acetal. Methylation of **72**, followed by hydrolysis of **74**, gave target **38** which could be fluorinated to give yet another target, **34**.

To prepare **72** for deoxygenation, we introduced a xanthate ester to provide **75**. Upon removing the acetal, **76** resided in the $^1C_4$ conformation, probably due to steric- or electron-withdrawing substituents.[88–90] The deoxygenation of **76** obtained target **39**. We needed to block position 3 to introduce the fluorine. However, **76** displayed surprising conformational flexibility, rendering the previous borinate methodology futile. Therefore, kinetic benzoylation at -35 °C,[88] reversed the selectivity to give **77** as the main product. Fluorination of **77** gave **78**, which after deoxygenation to **79** provided target **35** after deprotection.

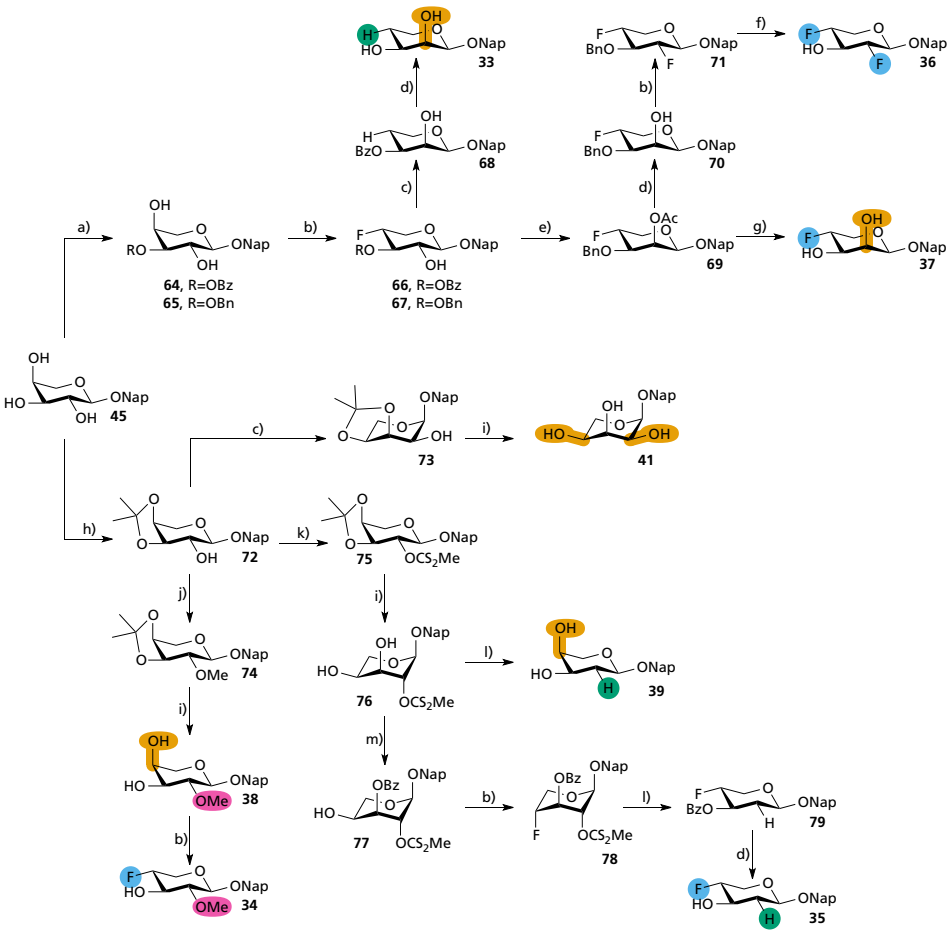

Scheme 3.4: Synthesis of targets via arabinose. Reagents and conditions: a) 2-aminoethyl diphenylborinate, BzCl, DIPEA, MeCN, **64** (64%) or 2-aminoethyl diphenylborinate, BnBr, KI, K_2CO_3, MeCN, **65** (57%); b) DAST, CH_2Cl_2, 40 °C, **34** (10%), **66** (22%), **67** (28%), **70** (61%), **78** (47%); c) DMSO, Ac_2O, MW 80 °C, then $NaBH_4$, MeOH, 0 °C, **68** (45% over two steps), **73** (75% over two steps); d) NaOMe (1M), MeOH, **33** (90%), **35** (28%), **71** (88%); e) Tf_2O, pyridine, 0 °C, then AcOH/DBU (12:6 eq), toluene, 90 °C, **69** (67%); f) HCl (conc. 22 eq), Pd/C (10 mol%), H_2 (1 atm), DMF, **36** (79%), g) HCl (conc. 22 eq), Pd/C (10 mol%), H_2 (1 atm), DMF, then NaOMe (1M), MeOH, **37** (78% over two steps), h) 2,2-dimethoxypropane, *p*-TsOH (cat.), DMF, **72** (95%); i) 70% AcOH, 60 °C, **38** (88%), **41** (59%), **76** (85%); j) NaH (60% disp. in mineral oil), MeI, DMF 0 °C, **74** (93%); k) NaH (60% disp. in mineral oil), CS_2, MeI, THF, 0 °C to r.t., **75** (87%); l) AIBN (cat.), H_3PO_2 in 1,4-dioxane, Δ, **39** (27%), **79** (18%); m) BzCl, pyridine, -35 °C, **77** (50%)

3.2.5 Synthesis of targets via lyxose

The lyxose pathways are depicted in Scheme 3.5. First, we protected **47** with an isopropylidene acetal to get **80**, from which the synthesis then diverged. We obtained target **29** by first methylating **80** and hydrolyzing the acetal of the resulting **81**. Similarly, the introduction of a xanthate ester on **80**, followed by hydrolysis of **82**, gave **83**. Neither borinate catalysis nor careful acylation rendered any suitable protecting group substitution on **83** due to conformational flexibility and modified reactivity. However, we envisioned the introduction of an acetate via orthoester hydrolysis, which opened to position 3 due to the conformational change. We expected this since orthoesters open via a combination of sterical and stereoelectronical factors to the axial position.[91–93] The crude product could then be fluorinated to yield **84**. Deoxygenation, followed by methanolysis, gave target **32**.

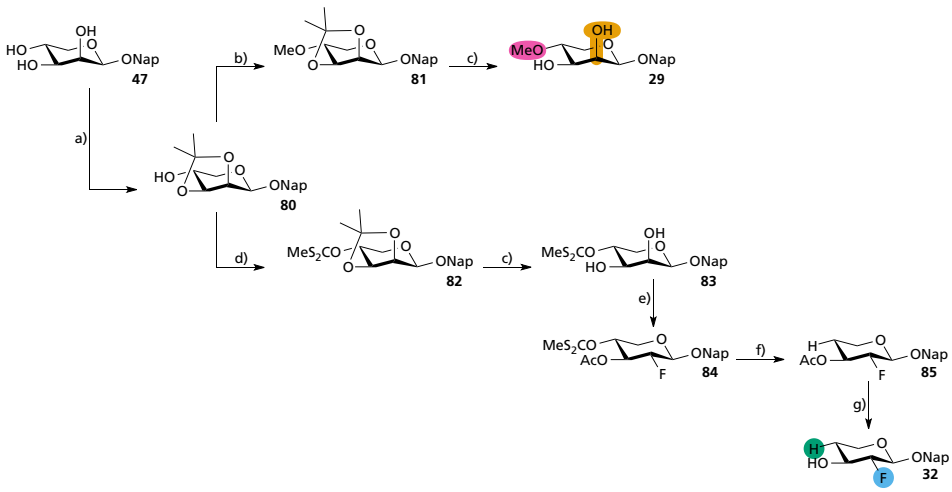

Scheme 3.5: Synthesis of targets via lyxose. Reagents and conditions: a) 2,2-dimethoxypropane, *p*-TsOH (cat.), DMF, **80** (96%); b) NaH (60% disp. in mineral oil), MeI, DMF 0 °C, **81** (86%); c) 70% AcOH, 70 °C, **29** (89%), **83** (95%); d) NaH (60% disp. in mineral oil), CS_2, MeI, THF, 0 °C to r.t., **82** (85%); e) Triethyl orthoacetate, *p*-TsOH (cat.), MeCN, then DAST, CH_2Cl_2, 40 °C, **84** (53% over two steps); f) AIBN (cat.), H_3PO_2 in 1,4-dioxane, reflux, **85** (69%); g) NaOMe (1M), MeOH, **32** (93%).

3.2.6 β4GalT7 assay

We investigated the 16 synthesized analogs as inhibitors/substrates in the β4GalT7 assay (Table 3.4), comparing them with the previous investigation.[39] Not surprisingly, none of the analogs showed any galactosylation, which we expected due to the absence of the free 4-OH in the proper orientation for galactosylation. More surprisingly, only 2 out of 16 compounds showed inhibition, namely **28** and **40** (25% and 30% respectively). Disturbing the hydrogen bonding by double substitution is clearly not well tolerated by the enzyme. Another recently published study, based on substituted xylosides with a methylumbelliferyl aglycon, presented similar results.[94]

Table 3.4: Inhibition of formation of GalXylNap by β4GalT7. Presented as the decrease of product formation compared to the absence of inhibitor, using **1** as the primer. Italicized values are monomodified analogs from the previous investigation.

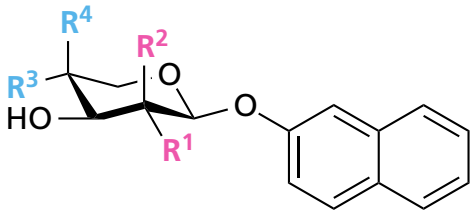

	R^1=OH	R^1=OMe	R^1=H	R^1=F	R^2=OH
R^3=OH	-	-	*11*	*43*	*52*
R^3=OMe	*14*	-	-	25	-
R^3=H	*64*	-	-	-	-
R^3=F	*9*	-	-	-	-
R^4=OH	-	-	-	30	-

3.2.7 Meta-analysis

Since the synthesis of the conceptually straightforward compounds was more complex than expected, we decided to make a meta-analysis and delve into the synthetic efforts towards the final compounds. We looked at a couple of parameters that seemed appropriate to explain synthetic complexity. ”Number of experiments,” which we defined as the number of unique experiments needed to unveil the final pathway. ”Number of synthetic steps” signifies the number of transformations in the final pathway. ”Yield” is the multiplication of individual yields in the final synthetic sequence, starting from **1**.

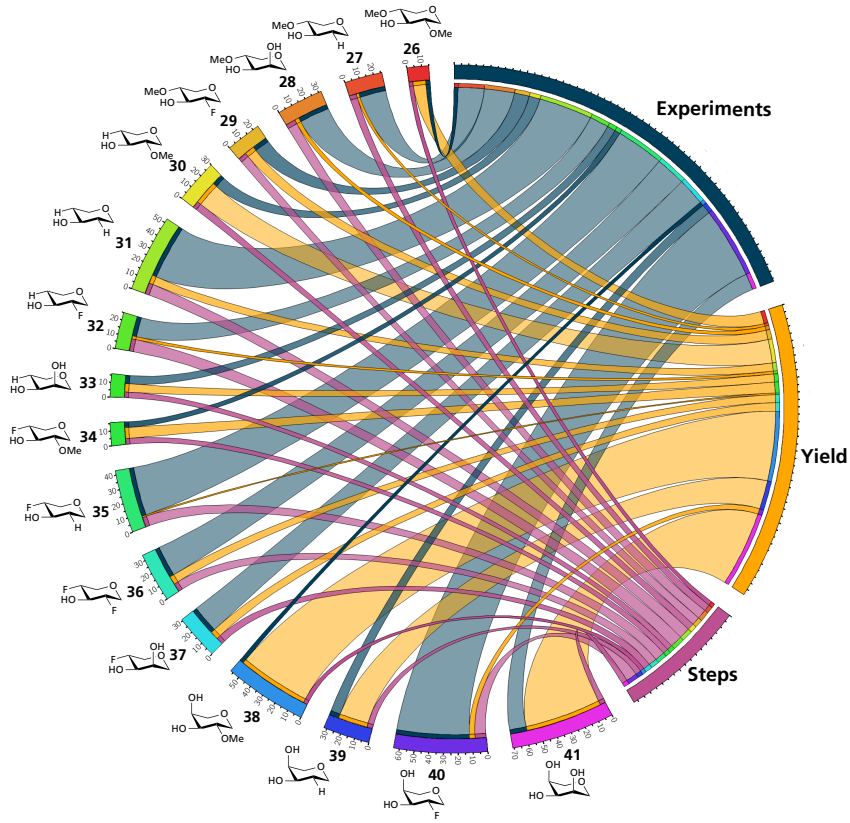

Figure 3.8: Meta-analysis of the synthetic work. The table is read by following the ribbons from the point of interest to the destination. The width of the ribbon is relative to absolute integers (wider=larger number), transparency is related to quartiles (lower quartile=less transparency). As an example, **39** has 7 experiments, 21% overall yield, and 4 synthetic steps.

Here, the data is represented in Figure 3.8 in a circular layout to make an interconnected visualization.[95] We reached most of the targets in a similar number of steps, ∼5-6, consistent with protecting group strategies. The three most high-yielding compounds were all arabinosides, with the apparent exception of **40**, the overall most challenging target to reach (57 experiments).

When comparing the total yield for the compounds, only four compounds surpass 10% in total yield. This low number indicates a bottleneck in most syntheses, and a common denominator for the lowest yielding targets is fluorination or deoxygenation. Especially combinations of the two transformations are complex since they required many experiments and were generally low yielding. In comparison to deoxygenations and fluorinations, methylations and epimerization are more straightforward.

3.2.8 Conclusions

We set out to investigate if doubly substituted xyloside analogs would make efficient inhibitors for β4GalT7, as a logical continuation to investigating monosubstituted xylosides. We found that the synthetic planning was far from straightforward and we needed to evaluate each of the 16 compounds individually. Only 2 out of 16 compounds showed any inhibition of β4GalT7, which is in line with findings from other groups, suggesting that the active site is very narrow, with precise hydrogen bond interactions required for binding. Therefore, making more than one substitution is not a suitable approach to make inhibitors.

3.2.9 Key findings in Paper II

The key points from Paper II and doubly modified xylosides are:

- Introducing double modifications of xylosides requires extensive synthetic planning and consideration.
- There is no synergistic effect seen in double modifications.
- We only observed minor/intermediate inhibition for two compounds, **28** and **40**.
- Meta-analysis emphasized the importance of choosing an appropriate starting material.

3.3 UDP-xylose constructs (Paper VII)

Most of the inhibitor design of xylosides for β4GalT7 has focused on modifications on the xylose moiety (Paper II, Section 1.4) with varying success. However, there are two binding sites in β4GalT7: one pocket for UDP-Gal with Mn^{2+} and one xylose binding pocket. These different sites are closely situated since β4GalT7's function is to galactosylate the xylose in the first step of the GAG biosynthesis (Sections 1.2 and 1.3). Since the most significant binding interactions come from the diphosphate, it is possible to envision an extension from xylose into the UDP-Gal binding pocket. We, therefore, hypothesized that by elongating the **1** scaffold with a UDP analog on position 4, it could be possible to achieve potent inhibition (Figure 3.9) of the enzymatic activity.

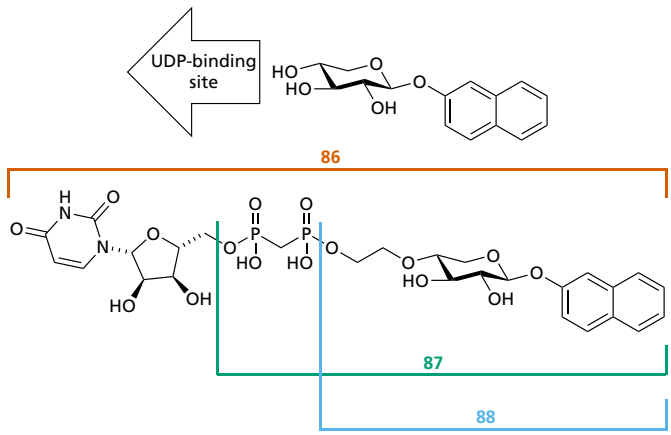

Figure 3.9: : Introducing different extensions to the xylose to find new binding interactions and create a new inhibitor type.

To mimic the potential transition state of the enzyme,[82,96] we then envisioned to probe for interactions starting from **86** and then removing fragments to see if there is a minimum epitope required for binding. **87** lacks the uridine moiety, while **88** lacks both uridine and bisphosphonate portions. We decided to use a more hydrolytically stable methylene bisphosphonate instead of a bisphosphate. Also, we decided to avoid a carbanionic approach,[97] due to the potential handling of very toxic intermediates, for instance, methyl phosphonic dichloride.[98]

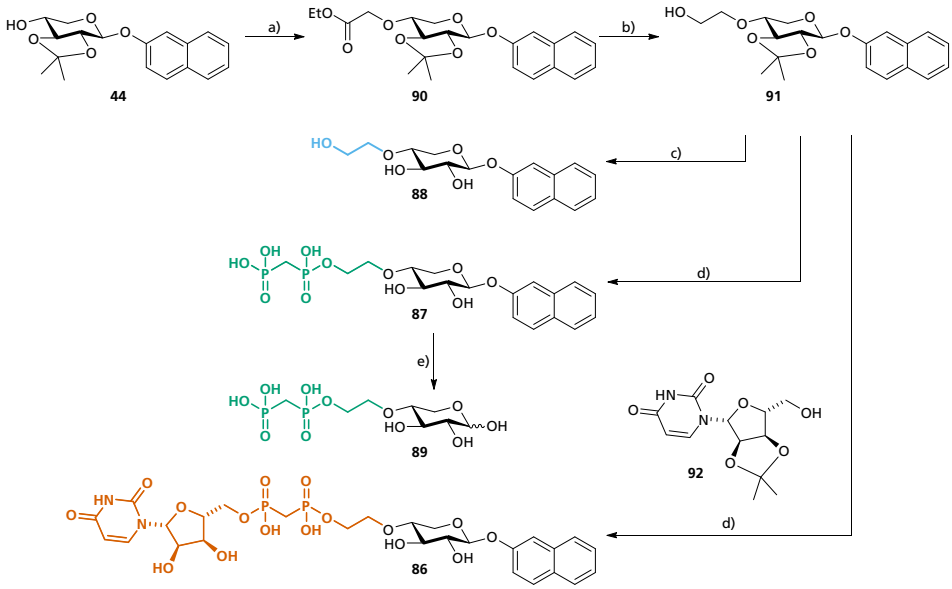

Scheme 3.6: Synthesis of the target molecules. Reagents and conditions: a) NaH (60% disp. in mineral oil), ethyl iodoacetate, THF, 0 °C, **90** (71%); b) $LiBH_4$, THF, 0 °C, **91** (78%); c) 70% AcOH, **88** (61%); d) $CH_2(P(O)Cl_2)_2$, $PO(OEt)_3$, DIPEA, 0 °C to r.t., then 70% AcOH, 55 °C, **86** (15%), **87** (8%); e) 1M HCl, MW 95 °C, **89** (67%).

3.3.1 Synthesis

The synthesis of the target molecules is shown in Scheme 3.6. We based the synthesis on a one-pot assembly, where the whole molecule was connected sequentially and then deprotected. First, starting from previously known **44** (Section 3.2.2), an alkylation with an α-haloester gave **90**, which upon reduction of the ester gave **91**. Next, to reach target **86**, **90** and known **92** —prepared by protecting D-uridine with an isopropylidene acetal[99]— were added successively to methylene bis(phosphonic dichloride). Finally, upon completion of the condensation, the target was hydrolyzed using acid to give the final compound **86**.

Similarly, we prepared target **87** with the same procedure but without the addition of **93**. Finally, we reached target **88** by acetal hydrolysis of **91**. Since we used methylene bis(phosphonic dichloride), a reactive electrophile, we observed over-addition of **91** and **92**, forming, in particular, **93** and **94** as sideproducts (Figure 3.10).

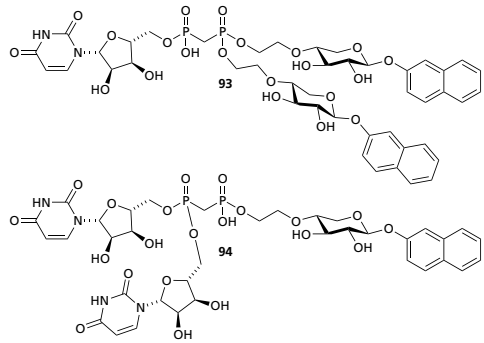

Figure 3.10: Sideproducts **93** and **94** observed during the condensations to reach **86**.

3.3.2 β4GalT7 assay

We investigated the targets as inhibitors of enzyme activity in the β4GalT7 assay (at a slightly lower concentration than previous inhibition studies). **87** did display inhibition, while **86** and **88** showed none (Figure 3.11, a). Also, **87** seemed to display concentration-dependent inhibition (Figure 3.11, b). However, we encountered complications with reproducibility. We discovered that **87** hydrolyzed slowly in acidic solution, forming the fragment **89** and 2-naphthol. It also seemed to form a precipitate with Mn^{2+} in the buffer. These factors are assumed to be the source of conflicting results regarding inhibition. In particular, barely any inhibition was observed when increasing the buffer strength for preparation of the stock solution of **87** (Figure 3.11, c). However, since we observed inhibition of β4GalT7, we decided to investigate the fragment **89** and 2-naphthol in the assay to see if the hydrolysis products were active.

We hydrolyzed **87** using HCl and microwave irradiation at 95 °C to obtain **89**.[†] Running the assay, we observed potent inhibition of the enzymatic activity (Figure 3.11, d). 2-naphthol also displayed inhibition, so it is of great interest to access its interactions as well. We reason that the lack of inhibition for **87** could be that the interactions with the naphthyl moiety counteracts the interactions of the bisphosphonate with the Mn^{2+}. Extending the aglycon linker could potentially alleviate this issue. Removing the naphthyl from **86** could also be interesting to investigate.

[†] At the time of writing, a more clear procedure is being established.

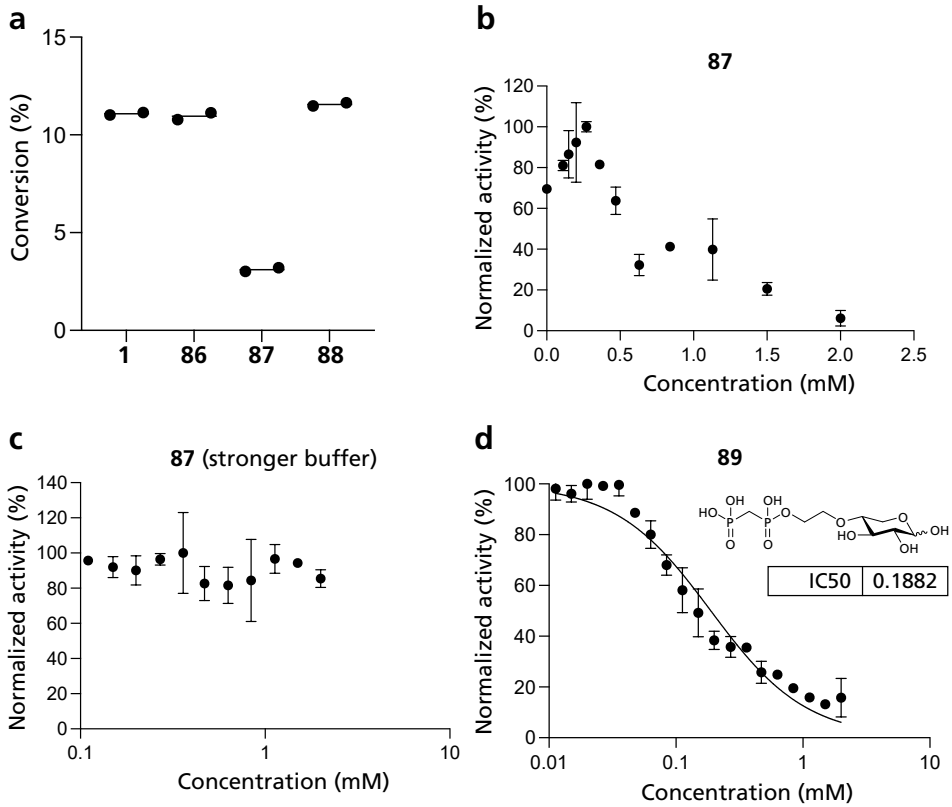

Figure 3.11: β4GalT7 assay results for UDP-xylose constructs. **a)** Comparison of **1**, **86**, **87**, and **88** at one concentration (1 mM). **b)** **87** displaying concentration-dependent inhibition (early data). **c)** Attempt to replicate findings with stronger buffer conditions. **d)** Assay with hydrolysis product **89** (same buffer conditions as **C**), obtaining an IC_{50} of 188 μM.

3.3.3 Conclusions

We set out to investigate if it was possible to make efficient inhibitors of β4GalT7 by extending the naphthoxyloside with a uridine-bisphosphonate moiety to access interactions in the UDP-Gal binding site, as well as finding a potential minimum binding epitope. We synthesized the different targets using a one-pot approach, condensing and deprotecting the different fragments without isolation. One compound, **87**, displayed concentration-dependent inhibition; however, closer investigations revealed that **87** was not the source of inhibition but rather its hydrolysis product **89**, reaching a low IC50 of 188 μM. Thus, **89** could potentially be a new class of compounds for inhibition of GAG biosynthesis.

3.3.4 Key findings in Paper VII

The key points from Paper VII and the UDP/bisphosphonate-xyloside constructs are:

- The synthetic strategy worked well to make asymmetric bisphosphonate molecules, skipping many protection, condensation, and deprotection steps.
- We potentially created a transition state analog **89** as a potent inhibitor of β4GalT7 activity, achieving an IC_{50} of 188 μM.
- The bisphosphonate is required for effective binding, coordinating strongly to the Mn^{2+}. However, the naphthyl also interacts strongly, potentially enough to pull the bisphosphonate in **87** away from Mn^{2+}.
- There is much potential to improve the binding efficacy of **89**. Modifying the structure to access the naphthol interactions should provide even stronger binding.

Chapter 4

Aglycon modifications

4.1 Deuterated naphtyl for mass spectrometry (Paper III)

As shown in the previous chapter, the β4GalT7 enzyme does not tolerate many modifications of the xylose moiety. Thus, in order to functionalize the primer, all modifications must be made in the aglycon. A simple yet effective alteration is using deuterium instead of hydrogen atoms. Deuterium is possible to distinguish from regular hydrogen due to its mass difference. Therefore, it has applications in chemical biology as a tracer or identifier.

Using **95**, with a deuterated naphthyl would simplify liquid chromatography-tandem mass spectrometry (LC-MS/MS) identification of fragments after being processed by enzymes since it would have a distinctive difference of +7. We, therefore, hypothesized that using a deuterated naphthyl aglycon on xylose would simplify MS analysis on cell primed GAGs (Figure 4.1).

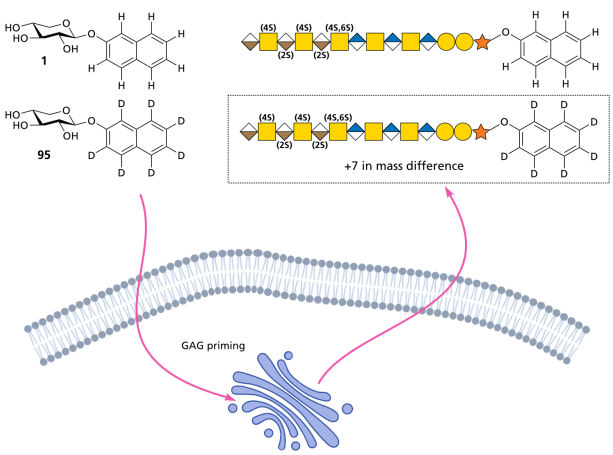

Figure 4.1: The concept of this study: utilizing a deuterium-labeled aglycon for simplifying MS analysis and enable linkage region differentiation.

This mass difference would then enable relative differentiation of fragments containing the linker region, in addition to information regarding disaccharide composition and structural differences of the primed GAG chain between different cell lines.

4.1.1 Target synthesis

The synthesis of target **95** is shown in Scheme 4.1. The short synthesis consisted of xylosylation of commercially available d_7-2-naphthol with peracetylated xylose **96**, followed by methanolysis of **97** to provide the final target **95**.

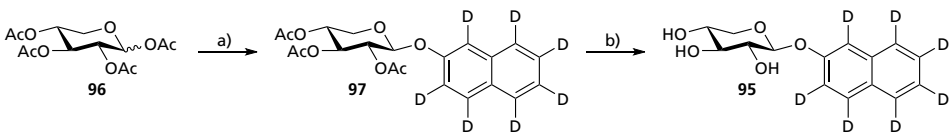

Scheme 4.1: Synthesis of deuterated **95**. Reagents and conditions: a) d_7-2-naphthol, $BF_3 \cdot OEt_2$, Et_3N, **97** (99%); b) NaOMe (1M), MeOH, **95** (60%).

Interestingly, the deuterated naphthyl showed hydrogen-deuterium exchange (Figure 4.2, left) after the reaction. The NMR spectra of **97** clearly showed an increase of ^{1}H-signal in the aromatic region after the reaction. A plausible mechanism for this could be an electrophilic aromatic substitution catalyzed by the Lewis acid (Figure 4.2, right). The amount of non-deuterated product was also estimated by HRMS and estimated to be a mixture of 48% D_7, 45% D_6, and 5% D_5. However, the amount of exchange was not of any significance for the actual biological testing.

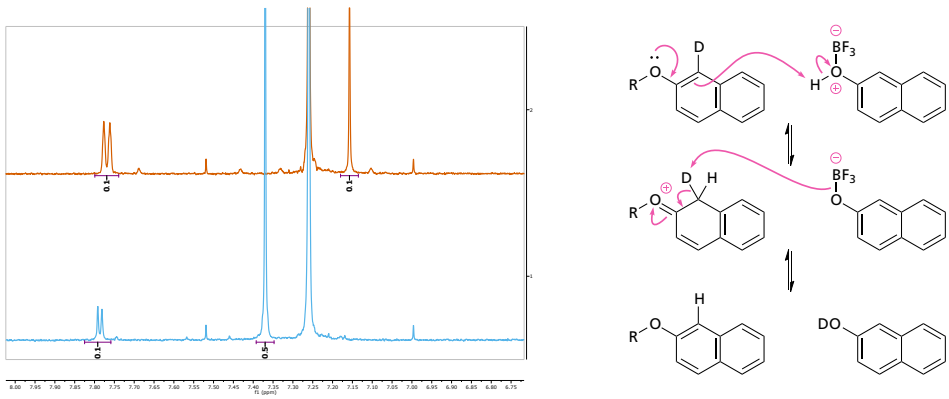

Figure 4.2: Left - ^{1}H-NMR showing deuterium-hydrogen exchange pre (top) and post (bottom). **Right** - Proposed mechanism for the exchange (only showing one deuterium for clarity).

4.1.2 Sample preparation and analysis

We incubated two cell lines with **1** and **95**, HCC70 (cell line of human breast carcinoma cells) and CCD-1095Sk (cell line of human breast fibroblasts), which we know produce GAGs with different compositions upon priming **1** and **2**.[100,101] The resulting xyloside-primed GAGs were subjected to enzymatic degradation using Chondroitinase ABC (Ch ABC), Chondroitinase AC-I/II (Ch AC-I/II), and Chondroitinase B (Ch B). The enzymes cleave the GAGs between the uronic acid and GalNAc moieties with different specificity; Ch ABC cleaves regardless of uronic acid, leading to complete disaccharide fragmentation. Ch A-I/II cleaves between GlcA and GalNAc, and Ch B cleaves between IdoA and GalNAc. This degradation allows an estimation of the types of disaccharide patterns present in the GAG chain.

This enzymatic degradation makes it possible to investigate more nuanced structural features of the disaccharides by using a combined LC-MS/MS method. The disaccharide fragments are separated by chromatography, followed by MS analysis and further fragmentation to reveal the structural features of the disaccharides based on the fragment ions. We then analyzed the fragmentation pattern with "SweetNET" to identify the parent glycans.[102]

4.1.3 Results

We obtained several findings regarding the structure of xyloside primed GAGs during this investigation. As a first analysis, the enzymatic degradation revealed the relative proportions of GAGs between the cell lines and the disaccharide composition between the two (Figure 4.3).

From this analysis, we can see that there is higher inclusion of IdoA in the GAGs from CCD-1095Sk cells than GAGs from HCC70 cells. From CCD-1095Sk cells, IdoA is present in 42% of the total CS/DS disaccharides, with approximately 1/3 as alternating/single units and 2/3 in blocks of the total amount. On the contrary, HCC70 primed GAGs contained less IdoA (11%).

Also, the disaccharide pattern revealed differences in sulfation; HCC70 contained mainly GalNAc sulfated in position 6, whereas CCD-1095Sk contained GalNAc primarily sulfated in position 4, with more disulfated disaccharides as well. These data indicate that xylosides primed GAGs from HCC70 have fewer complex structures since they have a lower proportion of IdoA and less disulfation.

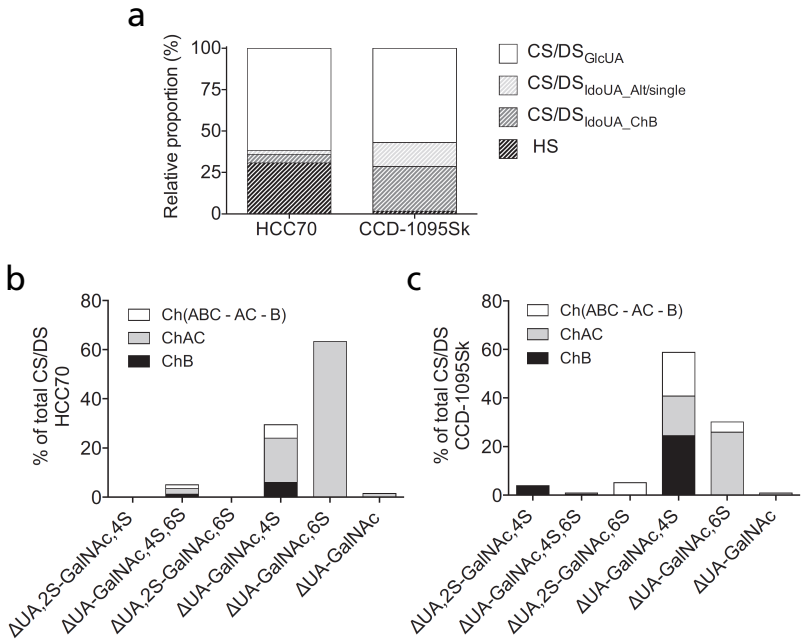

Figure 4.3: Proportions and disaccharide analysis of xyloside primed GAGs from HCC70 and CCD-1095Sk. **a)** - The relative proportion of HS and CS/DS in the two cell lines. **b)** and **c)** - The disaccharide analysis of HCC70 (*b*) and CCD-1095Sk (*c*), post enzymatic depolymerization indicated by the different bar colors.

We also treated cells with different fragments from HCC70 derived GAGs following chondroitinase treatment to see if the HS proportion and disaccharides or longer fragments of CS/DS were responsible for the observed cytotoxicity (not shown here, see Paper III). This experiment revealed that HS was not cytotoxic, and that cytotoxicity requires longer fragments. Furthermore, only disaccharides from Ch ABC treatment would not induce apoptosis.

The main purpose of the deuterated analog **95** was to make a relative quantification of linkage region fragments from the different cell lines. Mixing Ch ABC degraded GAGs from both HCC70 (primed with **95**) and CCD-1095Sk (primed with **1**) cell lines and analyzed with the LC-MS/MS method revealed that HCC70 primed linkage regions structures contained an N-acetyl neuraminic acid (Neu5Ac) residue (Figure 4.4, a). Interestingly, this modification was absent in the CCD-1095Sk primed GAGs, while other modifications showed similar proportions between the cell lines (Figure 4.4, b).

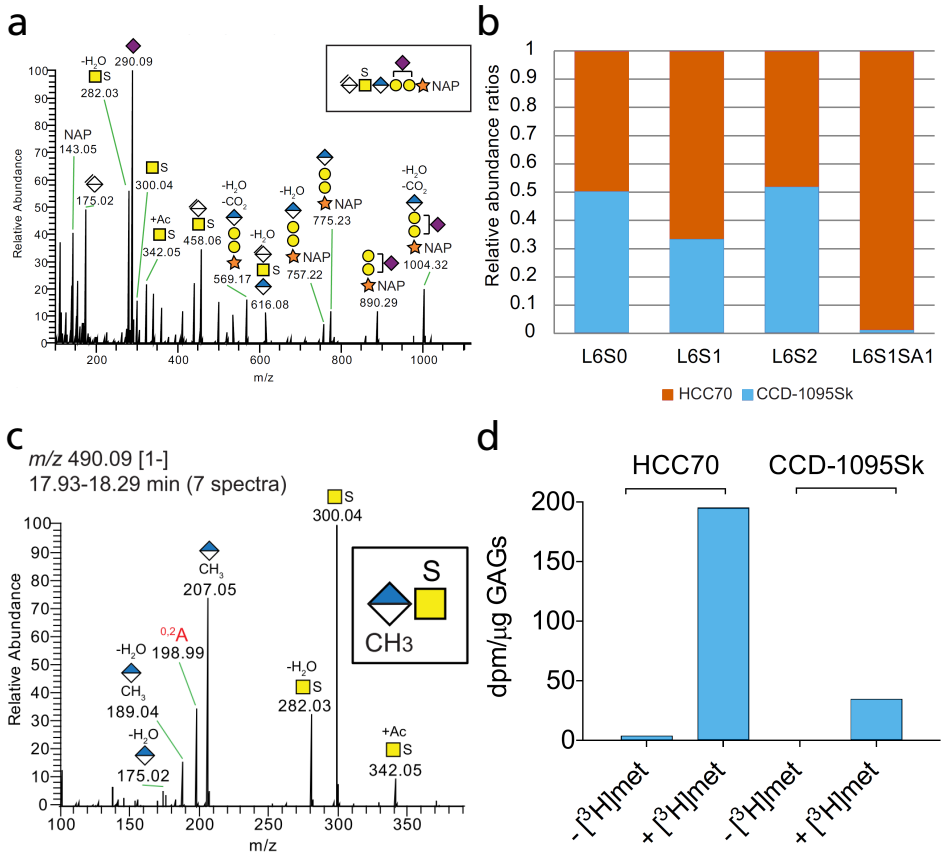

Figure 4.4: **a)** MS/MS spectrum of a precursor ion (*m/z* 753.19 [2-]) from a coupled LC-MS/MS analysis of xylosides primed GAGs from HCC70 cells. The top right shows the assigned glycan. **b)** Proportion of linker-region precursor ions modifications between HCC70 and CCD-1095Sk primed xylosides GAGs found in LC-MS/MS. L = amount of monosaccharides present, S = amount of sulfation, SA = Neu5Ac. **c)** MS/MS spectrum of a precursor ion corresponding to a methylated GlcA-SGalNac. **d)** Amount of radioactivity present in xylosides primed GAGs isolated from cells treated with or without radiolabeled [^{3}H]S-methylmethionine.

Treatment with a sialyltransferase inhibitor resulted in shorter GAGs where the Neu5Ac modification was more abundant, that is, the HCC70 cells (not shown here). However, this modification was only observed with Ch ABC or Ch AC-I/II degradation, suggesting that the Neu5Ac modification is associated with CS structures.

Looking for possible terminating structures at the non-reducing ends of the GAG chains revealed common motifs for both cell lines: a disulfated GalNAc residue as well as a saturated GlcA bound to a sulfated GalNAc. Also, a precursor ion corresponding to a methylated GlcA attached to a sulfated GalNAc residue was observed (Figure 4.4, c). To our knowledge, methylation as a termination of GAG synthesis has not previously been observed.

To verify, we supplied radiolabeled [^{3}H]S-methylmethionine to the two cell lines and measured the radioactivity from the isolated GAGs (Figure 4.4, d). Again, we observed a clear difference, with the HCC70 primed GAGs displaying a significant amount of radiolabeling. Thus, this experiment confirmed the MS/MS data while suggesting the general methyl donor S-adenosylmethionine as the active methylating reagent.

4.1.4 Conclusions

In this project, we set out to investigate more intricate structural features of xyloside primed GAGs from the two different cell lines HCC70 and CCD-1095Sk. We hypothesized that a xyloside derivative containing a deuterated aglycon would facilitate MS analysis by clear differentiation of mass, which assists in quantifying differences in linker-region structures where xylose is present. We discovered that the GAGs differed in HS and CS/DS and that the HS population was not responsible for cytotoxicity. In addition, the HCC70 cells primed GAGs contained less IdoA and less disulfated disaccharides than CCD-1095Sk cells, showing a difference in their disaccharide composition and sulfation pattern.

We also observed new modifications in GAG biosynthesis when using a novel LC-MS/MS approach. We observed the addition of a Neu5Ac residue to the linker region when utilizing the deuterated xyloside **95**. This modification also seemed to influence the biosynthesis. Also, we observed a previously unseen terminal methylation. Both modifications were present in HCC70 primed GAGs and not in CCD-1095Sk primed GAGs. Therefore, utilizing deuteration in the naphthoxylosides enables differentiation and facilitates MS analysis.

4.1.5 Key findings in Paper III

The key points from Paper III and the xyloside containing a deuterated naphthyl:

- Normal xylosylation conditions lead to loss of deuteration in the aglycon of **95**. This loss possibly occurs through an electrophilic aromatic substitution aided by Lewis acid.
- The deuterated naphthyl aglycon allows for quantifying linker region fragments by mass spectrometry and allows the identification of novel linker region modifications.
- Using **1** and **95**, we identified that GAGs from HCC70 and CCD-1095Sk can contain very different modifications.
- GlcA and IdoA are both required for GAG cytotoxicity when primed on exogenous xylosides.

4.2 A fluorescent tool for GAG intracellular localization (Paper V)

One of the most used techniques for the analysis of biochemical interactions is fluorescence microscopy. Fluorescence is a technique based on the absorption of light, followed by emission at another wavelength which is then detected and measured. This technique is a non-destructive way of analyzing certain biomolecules, which is also very specific due to the particular wavelengths used.

Being able to visually localize the xyloside primed GAGs in the cell would be a practical tool to study the GAGOsome hypothesis. The hypothesis says that multiple GAG processing enzymes co-localize in Golgi subcompartments, influencing the structures produced.[103] We, therefore, hypothesized that we could use a fluorescent aglycon to visualize the localization and processing of GAGs in cells (Figure 4.5).

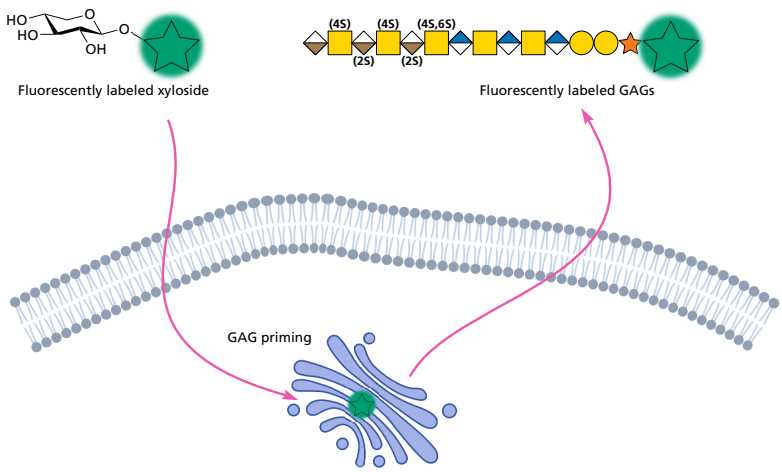

Figure 4.5: Concept of this study: Introduction of a fluorescent xyloside to probe localization in cells.

For this approach to work, the xylosides must be able to cross the cell membrane and then be able to initiate GAG synthesis via β4GalT7. We envisioned to use a small fluorophore to facilitate this transport while keeping the polarity as low as possible. Several guidelines for cellular uptake exist, with total polar surface area seemingly an important factor for passive absorption.[104–107] One guideline is that the molecule should have a suitable partition coefficient (logP) value,[†] similar to a compound that exhibits cellular uptake.

[†] LogP is a ratio of concentrations of a compound between two immiscible solvents at equilibrium, such as water and 1-octanol. Therefore, it is a measure of lipophilicity and therefore an estimate of how probable it is to pass a lipid bilayer such as the cell membrane.[108]

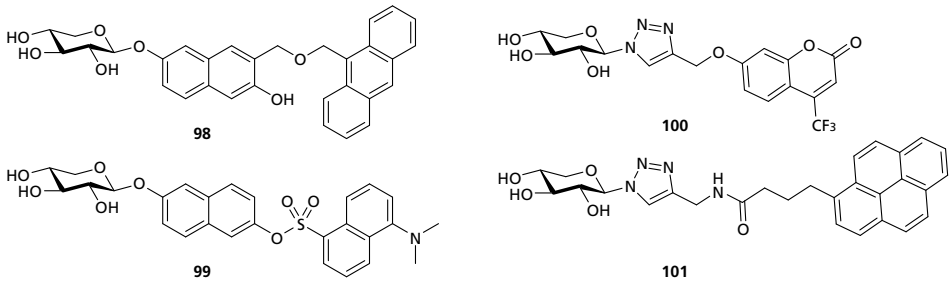

Figure 4.6: Previous attempts to make fluorescent xylosides.

There have been previous attempts to design fluorescent xylosides for GAG priming in cells (Figure 4.6).[49,50,109] These conjugates could enter cells but did not initiate GAG biosynthesis (except for **100**, which did display priming of GAGs and could be analyzed using fluorescence). Authors hypothesized that the aglycons were too bulky, but there were no further suggestions why GAG elongation did not initiate or was terminated early.

With this in mind, we decided to make a series of xylosides with varying linkers and a 1,5-dithioxyloside version to investigate in the β4GalT7 assay and to visualize them in cells (Figure 4.7). We based this on the observation that increased linker lengths improve substrate capability,[40] and the previous investigation regarding endo/exocyclic substituted xylosides (Section 3.1).

We decided to use PacificBlue™ (PacBlue), a coumarin-based fluorophore recently developed and used in biological investigations.[110–114] Our rationale for choosing this fluorophore was twofold: coumarin-containing xylosides are well-known to prime GAG-biosynthesis, and its relatively small size would increase the chance of cellular uptake. Furthermore, it exhibits a high quantum yield in water.[115,116]

4.2.1 Synthesis of targets

The synthesis of the targets is shown in Scheme 4.3. PacBlue is commercially available as an NHS-ester but is very expensive.† There is an optimized route enabling multigram synthesis published, which we utilized to make a significant amount of fluorophore available for synthesis (Scheme 4.2).[111] Using commercially available 2,3,4,5-tetrafluorobenzoic acid makes it possible to obtain the PacBlue carboxylic acid in 7 steps with only one chromatographic step.

† 383€ / 5 mg at the time of writing.

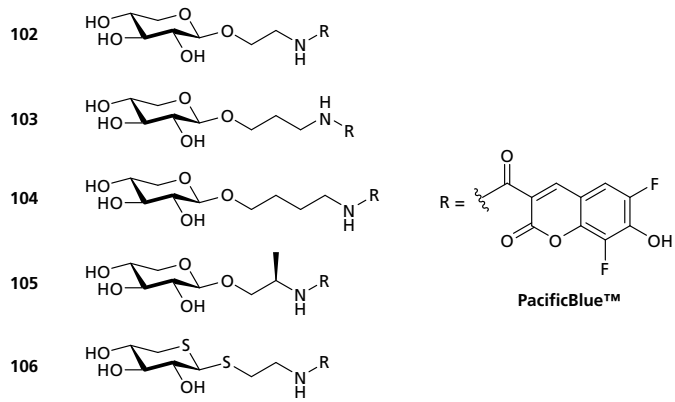

Figure 4.7: Synthetic targets for this study, containing the fluorescent coumarin PacificBlue™.

We employed conventional carbohydrate chemistry; starting from **96**, xylosylation using $BF_3 \cdot OEt_2$ gave the protected linker intermediates **107**, **108**, **109**, and **110**. Next, hydrogenolysis of the Cbz protecting group provided the free amines **111**, **112**, **113**, and **114**, then coupled with the carboxylic-acid containing PacBlue fluorophore to yield **115**, **116**, **117**, and **118**. Methanolysis then provided the final targets **102**, **103**, **104**, and **105**.

We did not have any success synthesizing **106** under similar conditions, i.e., peracetylated donor and $BF_3 \cdot OEt_2$. Therefore, we modified the strategy to use **21** as the donor and a commercially available Boc-protected amine linker. With the same conditions as for previous thioxylosides (Section 3.1), we obtained **119** as an α/β mixture (1:2). Hydrolysis with LiOH then gave **120**, followed by Boc deprotection with HCl/EtOH to give **121**. Coupling with commercially available PacBlue containing a succinimidyl ester yielded the final compound **106**. We re-evaluated the synthesis pathway after we synthesized enough **106**, hence the change in methodology.

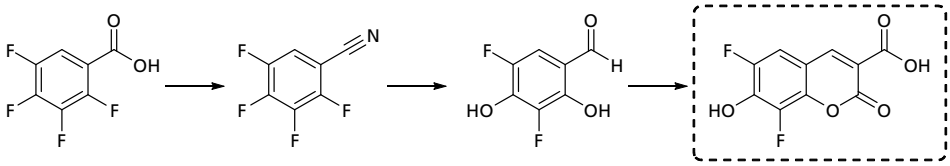

Scheme 4.2: Synthesis of Pacific Blue, as described by Lee et al.

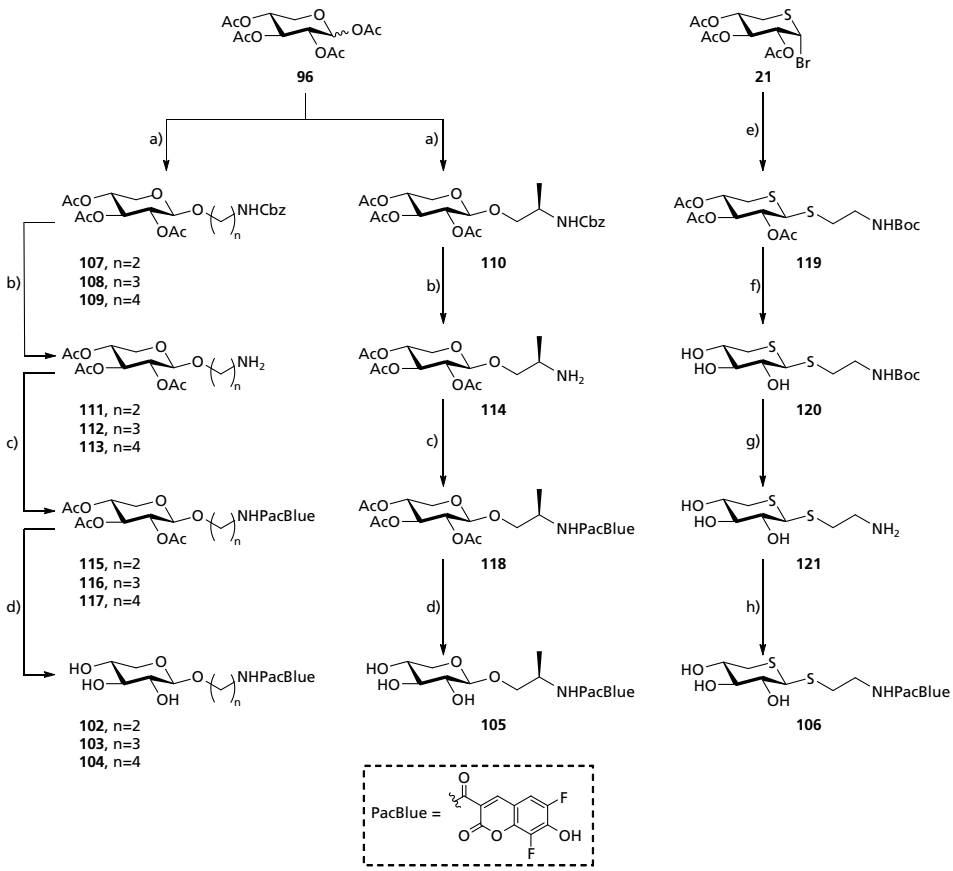

Scheme 4.3: Synthesis of target fluorescent xylosides. Reagents and conditions: a) Glycosyl acceptor, $BF_3 \cdot OEt_2$, MeCN, **107** (20%), **108** (20%), **109** (14%), **110** (21%); b) Pd/C (10%), H_2 (1 atm), MeOH, **111** (quant.), **112** (96%), **113** (94%), **114** (62%); c) PacBlue-COOH, EDC, HOBt, Et_3N, **115** (36%), **116** (40%), **117** (58%), **118** (55%); d) K_2CO_3, MeOH, **102** (98%), **103** (96%), **104** (96%), **105** (73%); e) Boc-protected thiol linker, ZnO-$ZnCl_2$, toluene/MeCN (1:1), MS 3Å, 60 °C, 2h; **119** (40%, β/α 2:1); f) LiOH, MeOH, **120** (98%, β/α 2:1); g) HCl (1M), EtOH, **121** (52%); h) PacBlue succinimidyl ester, DIPEA, DMF, **106** (46%).

4.2.2 Comparison of logP values

To estimate the possibility of cellular uptake of the final compounds, we evaluated them regarding their lipophilicity. We then utilized gradient HPLC retention times as an estimation for logP values in biological systems.[117,118]

We compared the targets compounds to **1**, which displays cellular uptake and priming (Figure 4.8). Lipophilicity increased with longer linker length, which we expected. The compound displaying the most similar lipophilicity to **1** is the 1,5-dithioxyloside **106**. The sulfur atoms seem to cancel out the polar PacBlue moiety to a large degree.

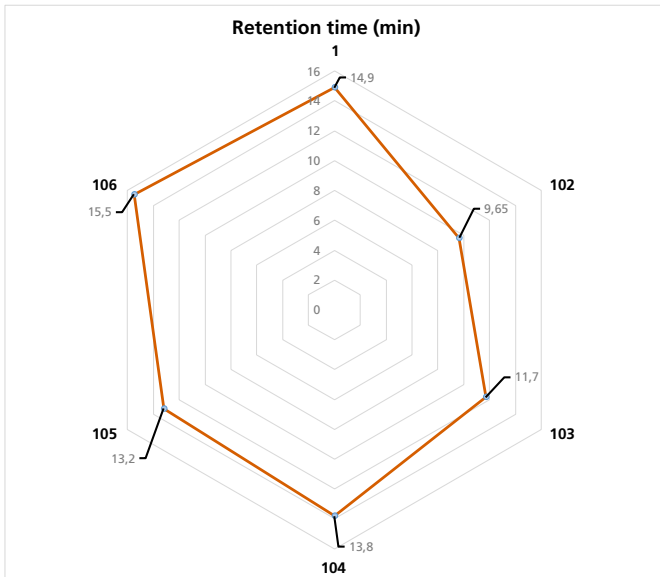

Figure 4.8: LogP comparison of the target compounds.

4.2.3 β4GalT7 assay

We evaluated the compounds as substrates in the β4GalT7 assay (Figure 4.9, Table 4.1). They all displayed galactosylation while also displaying significantly faster kinetics than **1**, **106** being the most efficient. This result is in agreement with previous data obtained for thioxylosides (Section 3.1). In addition, all compounds displayed substrate inhibition above a concentration of approximately 0.5 mM.

We also decided to investigate some previous fluorescent xylosides that had failed to initiate GAG biosynthesis (**98** and **99** to see if they were β4GalT7 substrates. In agreement with previous results,[50,109] these compounds were not galactosylated in the β4GalT7 assay.

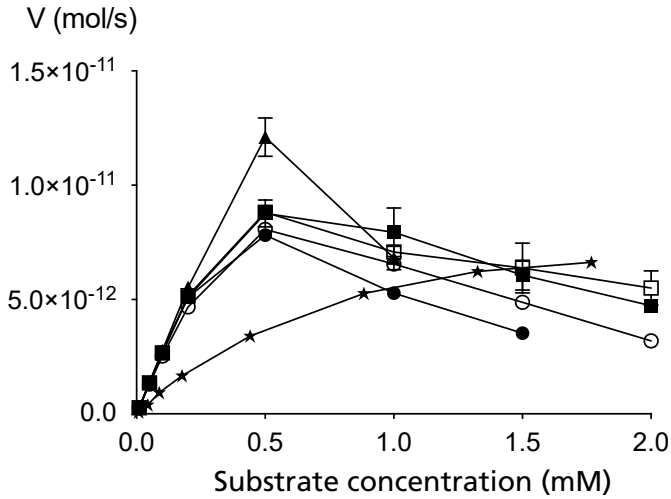

Figure 4.9: Michaelis-Menten representation of β4GalT7 activity with the investigated xylosides. **1** (star), **102** (filled circle), **103** (hollow circle), **104** (filled square), **105** (hollow square), and **106** (triangle).

Table 4.1: Kinetic parameters for β4GalT7 galactosylation.

Substance	Structure	K_m (mM)	V_{max} (pmol s^{-1})	k_{cat} (s^{-1})	k_{cat}/K_m ($mM^{-1}\,s^{-1}$)
102	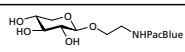	0.39	14.1	4.4	11.3
103	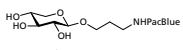	0.55	17.0	5.3	9.7
104	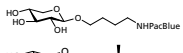	0.57	18.9	5.9	10.3
105	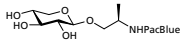	0.57	19.0	6.0	10.4
106	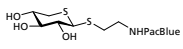	2.2	65.8	20.6	9.3

4.2.4 Cellular uptake, priming, and localization

Knowing that the xylosides could act as substrates for β4GalT7 and displaying similar logP values as a known primer, we investigated **102**, **104**, and **106** in vitro, using adenocarcinomic human alveolar basal epithelial cells (A549) cells to see if they were able to prime GAG biosynthesis. The actin skeleton in the A549 cells was tagged with green fluorescent protein (GFP), using CRISPR/Cas9 methodology to aid visualization of the uptake and localization of the xylosides in the cells. Also, we investigated peracetylated versions since acetylation is a known method to increase cellular uptake of carbohydrates.[119,120]

None of the xylosides primed full-length GAGs. However, when analyzing the cell medium, short products corresponding to a partially processed GAG chain were observed using size-exclusion chromatography.

Confocal microscopy was performed on **102** to visualize the uptake and localization in the cellular compartments. After including Golgi and lysosome trackers, we observed that **102** derivatives were located mostly perinuclear and did not co-localize with either Golgi or in lysosomes (Figure 4.10). Next, the cell cytoplasm was analyzed to identify the observed signals, after which mostly unprocessed **102** was discovered. Thus, we suspect that the charge on the fluorophore seriously hinders the transport into Golgi.

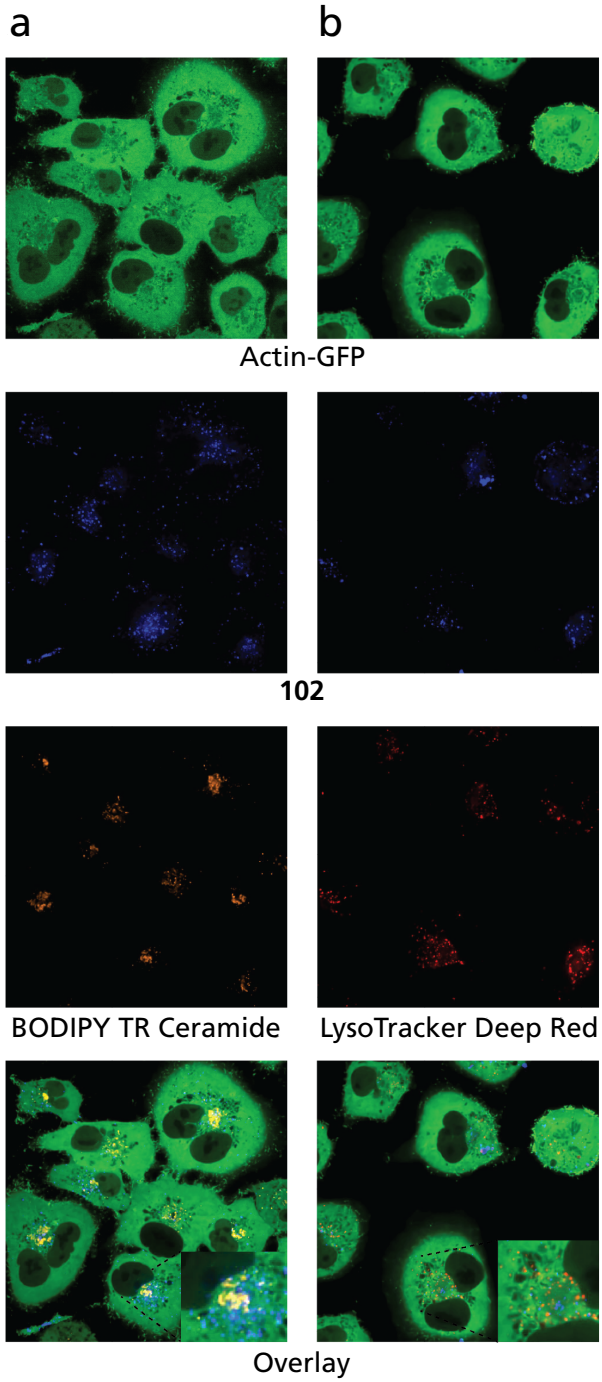

Figure 4.10: Confocal microscopy imaging of the localization of **102**-primed products in A549 cells treated with 0.1 mM **102**. Column **a**: Experiment using BODIPY TR Ceramide, which localizes to the Golgi apparatus. Column **b**: Experiment using LysoTracker Deep Red which targets lysosomes.

4.2.5 Conclusions

In this project, we investigated the possibility of using a fluorophore coupled to a xylose moiety to visualize the GAG biosynthesis inside the cell. We synthesized five different analogs containing the PacificBlue™ fluorophore, and we showed that they were galactosylated by β4GalT7, as well as having β4GalT7, and have suitable logP values for cellular uptake. **102**, **104**, and **106** were taken up by cells but did not prime full-length GAGs, only short disaccharide fragments. Furthermore, **102** was visualized by confocal microscopy, revealing that it did not co-localize in Golgi or lysosomes. Thus, transport into and processing in Golgi is not possible using this type of fluorophore. Most likely, the charge present in the fluorophore limits the uptake into Golgi.

4.2.6 Key findings in Paper V

The key points from Paper V and the fluorophore-containing xylosides are:

- First, PacBlue-containing xylosides does act as substrates for β4GalT7.
- The introduction of two sulfur atoms counteracts the polar coumarin fluorophore, which could be a valuable technique for logP alterations.
- The compounds were taken up by cells but not processed to full-length GAGs.
- Golgi uptake of exogenous xylosides seemingly depends on the charge present.
- We most likely need to introduce the fluorophore after priming to obtain fluorescent GAGs primed on xylosides; since common fluorophores are generally charged or very large, which would hinder uptake into Golgi.

4.3 Nitrogen-containing linker for functionalization (Paper IV and VI)

An advantageous property to include in biomolecular tools is a ”handle,” allowing modifications to the tool for different experimental setups. For example, **2** does prime GAG biosynthesis and contains a hydroxyl in the aromatic aglycon; it could be possible to add an extension that would include a handle for further functionalization.

We hypothesized that the introduction of a nitrogen-based functional group, such as an amine or an azide, would allow xyloside scaffold **2** to be further modified after cellular priming to be analyzed by biophysical techniques (Figure 4.11). Another advantage is that the primed GAG chains will be cell-specific, which could be of importance, depending on the scientific question asked.

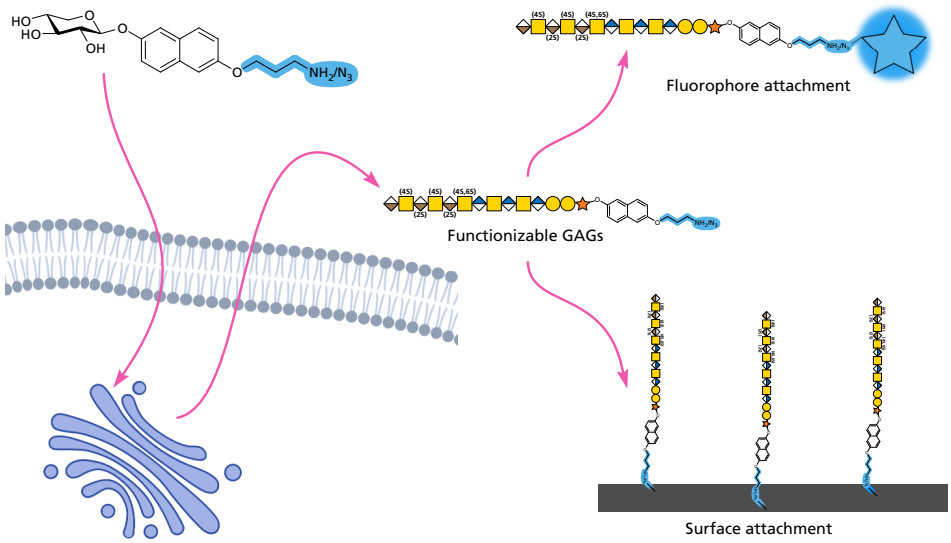

Figure 4.11: The concept of this study. Adding a nitrogen-containing linker to **2**, followed by cellular priming, could be used to investigate by biophysical means. For example, introduction of a suitable fluorophore or surface functionalization.

There are two principal ways of conjugation with the amine: the primed xyloside can react with an activated carboxylic acid or be transformed via reductive amination to form the desired conjugate. In comparison, the azide group reacts via a 1,3-dipolar cycloaddition.

This reaction is either copper- or strain-catalyzed to form the conjugate. Also, the azide can be reduced to an amine if the situation requires it. In principle, this allows the GAG primed xyloside to be attached to various structures if an appropriate carboxylic acid or alkyne is present.

4.3.1 Synthesis of targets

We used a linear synthetic strategy with a late divergence to reach amino target **122** and azide target **123** (Scheme 4.4). We started from peracetylated **124**, achieving a monodeprotection of the aromatic hydroxyl group using a mixture of NH_4OAc, MeOH, THF, and water under mild heating to give **125**. Alkylation of **125** introduced a spacer, followed by hydrolysis of resulting **126** using 1% HCl in MeOH to give **127**.

To allow the synthetic divergence, the free alcohol **127** was mesylated to give **128**. Then, to reach the amino-functionalized target, **128** was reacted in a Gabriel synthesis using microwave heating to give **129**. Lastly, we used a sequence of NaOMe, $NaBH_4$, and AcOH to give target **122**.[121] For the azido functionalized target, we introduced the azide on **128** using NaN_3 and microwave heating to provide **130**. In the end, methanolysis of the protecting acetates gave target **123**.

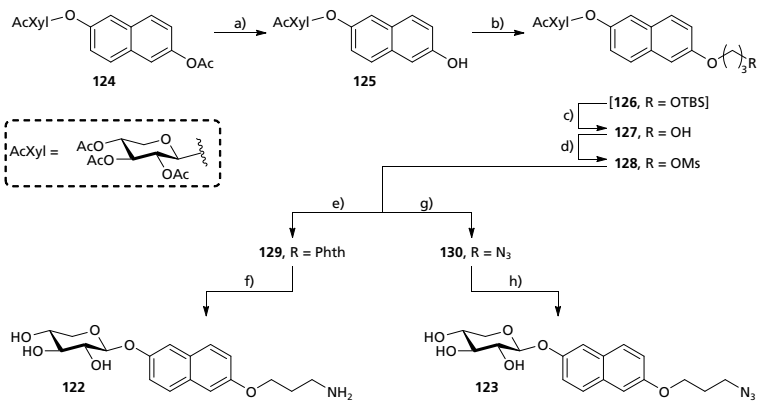

Scheme 4.4: Synthesis of xylosides containing a functionizable linker. Reagents and conditions: a) NH_4OAc, THF, MeOH, H_2O, 40 °C, **125** (84%); b) 3-(*tert*-butyldimethylsilyloxy)propyl bromide. K_2CO_3, DMF, 40 °C; c) HCl, MeOH, **127** (63% over two steps); d) MsCl, pyridine, 0 °C to r.t., **128** (89%); e) KPhth, DMF, MW 75 °C, **129**; f) NaOMe, MeOH, then $NaBH_4$, *i*-PrOH, H_2O, then AcOH, 80 °C, **122** (66% over three steps); g) NaN_3, DMF, MW 90 °C, **130** (88%); h) K_2CO_3, MeOH, **123** (84%).

We attempted to synthesize targets with shorter linker lengths, but these turned out to be unstable or surprisingly challenging to get satisfactory pure for testing. Azide functionality close to nucleophiles in the presence of Brønstedt/Lewis acids can react in many types of reactions such as rearrangements, or cyclizations, with the loss of N_2 gas.[122] This could explain the difficulty in obtaining the shorter lengths since we use Lewis acids in conventional carbohydrate chemistry to attach the aglycon, which could present an opportunity for the azide to react with the aromatic system of the aglycon (Figure 4.12).

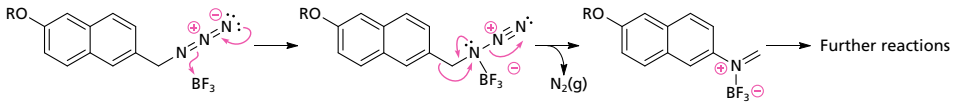

Figure 4.12: A potential mechanism for formation of side products during xylosylation with $BF_3 \cdot OEt_2$.

4.3.2 β4GalT7 assay

We evaluated **123** as a substrate in the β4GalT7 assay. It was galactosylated and displayed similar kinetics as **1** (Figure 4.13).

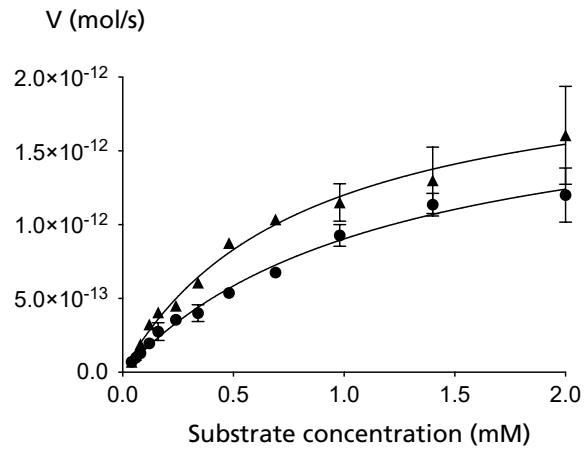

Figure 4.13: β4GalT7 kinetic profile for **123** (triangle) compared to **1** (square).

4.3.3 Biological studies

Recently, the Clausen group at the University of Copenhagen created a library of cell types where they knocked out or knocked in different enzymes responsible for GAG biosynthesis. This work resulted in the possibility of using the different cell types for investigating GAG epitopes by employing, for instance, flow cytometry (see Figure 4.14). Furthermore, **122** primed GAG biosynthesis in these cells and showed its usefulness as a tool to produce distinct GAG structures. These structures could potentially create, for instance, microarrays for analyzing interactions in a 96-well plate.

They observed that the resulting types of GAGs obtained with **122** were in principle the same as the result from **1**, but with a slightly different priming pattern. Worth noting is that **122** was not used to investigate a specific scientific question but to add another facet to the GAGomes capability.

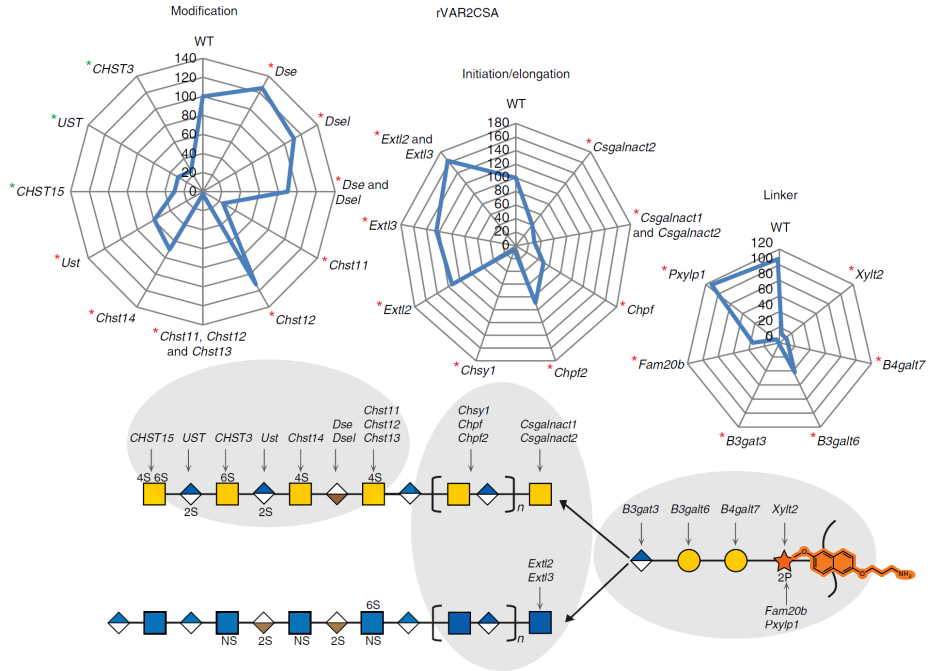

Figure 4.14: A modified picture illustrating the potential use of GAGome primed xylosides **122**. The illustration shows the recombinant VAR2CSA experiment in Paper IV with **122** superimposed (in orange) to illustrate the possible GAG structures using the GAGome. Radar graphs show fluorescence intensity; lower values mean weaker binding (WT is assigned 100). Names refer to enzymes involved in the GAG biosynthesis.

123 containing the azide is, in principle, a very similar molecule to **122**. However, the azide is a more flexible and biocompatible functional group, which could be an advantage. Firstly, we incubated A549 cells with **123** to prime soluble GAGs. After that, we reacted a fluorophore containing a dibenzocyclooctyne (DBCO-Alexa Fluor 647) with the GAGs in strain-catalyzed cycloaddition. Finally, the conjugated GAGs were purified using ion-exchange chromatography and analyzed with fluorescence-coupled size-exclusion chromatography.

We observed the presence of conjugated GAGs, verifying the functionality of the azide linker while simultaneously proving the concept. Secondly, using the same principle, **123** primed GAGs from lung fibroblasts were biotinylated via the azide and attached to an SPR sensor chip coated with streptavidin. Finally, kinetic studies with hepatocyte growth factor (HGF) revealed a K_D of $14 \cdot 10^{-12}$ between the GAGs and HGF ($k_a = 1.31 \cdot 10^6$ M/s and $k_d = 18 \cdot 10^{-6}$ M/s).

We also tried to introduce a tetramethylrhodamine (TAMRA) fluorophore before GAG priming while using confocal microscopy to visualize the localization of the xyloside constructs (similarly to Paper VI, section 4.2.4). So, the **123** was labeled

with TAMRA using a cycloaddition and administered to A549 cells. Unfortunately, no priming of GAGs was observed (in line with previous observations in Paper VI, 4.2.4). Still, the constructs were visible by confocal microscopy, demonstrating its potential usefulness. The results can be seen in Figure 4.15.

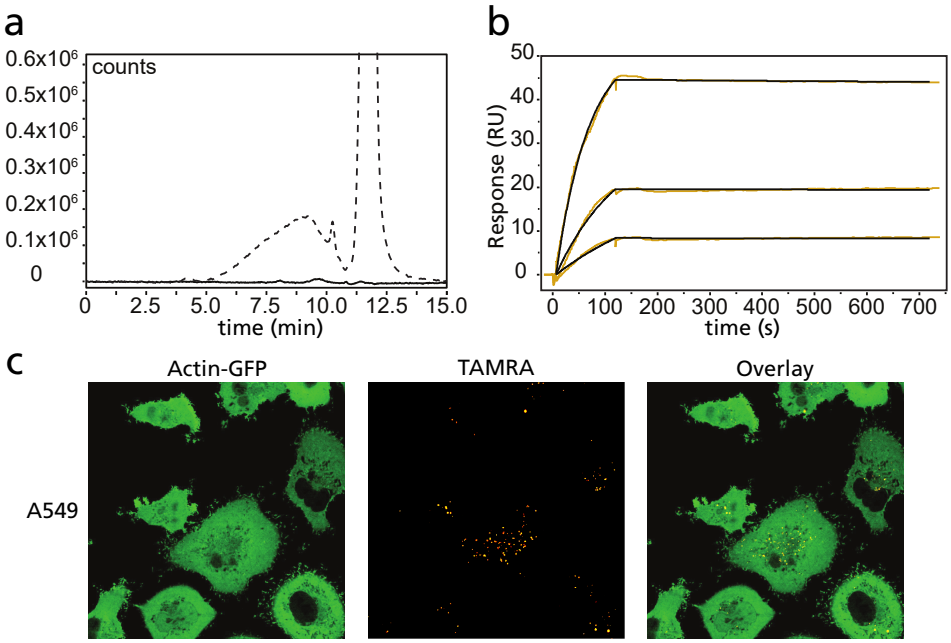

Figure 4.15: Verifying the capabilities of **123**. **a)** Chromatogram of cell medium before (solid line) and after (dashed line) click reaction between **123**-primed GAGs and an Alexa Fluor 647 fluorophore. The broad peak between 5-10 min corresponds to xyloside-primed GAGs, with excess fluorophore present at 12 min. **b)** SPR sensorgram of the interaction of **123**-primed GAGs and HGF at 3, 6, and 12 nM, demonstrating surface functionalization. **c)** Confocal microscopy image of A549 cells treated with **123** conjugates with TAMRA. Compounds were taken up and localized to the perinuclear region.

4.3.4 Conclusions

This project explored GAG-priming xylosides containing a linker where we could introduce new functionality. Mainly, we synthesized two different analogs: **122** with an amine group and **123** with an azide group. Both compounds could prime GAG biosynthesis. Furthermore, we used **122** in connection with a newly created cellular library, which could synthesize GAGs with defined structures for microarray assembly. GAGs primed on **123** could be modified with fluorophores, visualized by confocal microscopy, and attached to an SPR sensor chip with subsequent kinetic analysis of an HGF binding partner. These xylosides could therefore serve as tools to answer hypotheses regarding GAG interactions and biosynthesis.

4.3.5 Key findings in Paper IV and VI

The key points from Papers IV and VI and the aglycon functionalized xylosides are:

- Linker length is important when placing azides close to an aromatic moiety as side reactions are possible.
- The synthesized xylosides can function as primers for GAG-biosynthesis (**123** does act as a substrate for β4GalT7, demonstrated in vitro).
- Utilizing the GAGome, **122** showed that it is possible to prime specific GAG structures and potentially assemble them into microarrays.
- We successfully modified the azide linker on **123** and used several different biophysical techniques (fluorescence, confocal microscopy, SPR) as a proof of concept.
- These xylosides could answer questions using cell-specific GAGs, which is difficult using commercially available material.

Chapter 5

Conclusions and Future Prospects

To conclude this thesis work, we managed to verify several of the hypotheses proposed in the introductory chapter by synthesizing several different xylosides modified in the aglycon of the xylosides or the actual carbohydrate.

We can conclude the following regarding xylose modifications:

- It is possible to influence the priming kinetics by altering the endo/exocylic heteroatoms. Introducing one or two sulfur atoms led to much improved kinetic parameters, most likely via aromatic stacking interactions that lower K_m (Paper I).
- Substituting multiple hydroxyls in xylose does not create efficient inhibitors of β4GalT7. Instead, we need to target other parts of the xylosides or the active site to make efficient inhibitors (Paper II).
- Creating UDP-xyloside constructs did make an efficient inhibitor, however, not as a naphthoxyloside as imagined. The structure needs to be optimized, but the strategy works (Paper VII).

Also, we can conclude the following regarding xylosides aglycon modifications:

- Using a deuterated naphthyl does simplify MS analysis of cell-primed GAGs by allowing linker region assessment after enzymatic degradation. The mass difference is enough for a clear distinction and enables the identification of new biosynthetic modifications (Paper III).
- Using a coumarin fluorophore as an aglycon did allow confocal microscopy studies of xylosides taken up by cells. However, we did not observe any priming of GAGs. So to visualize GAGs, the fluorophore must be introduced after the biosynthesis (Paper V).

- Using xylosides with dihydroxynaphthalene aglycons containing a linker with either an amine or an azide did allow for functionalization of cell primed GAGs. We could prime them using the GAGome cell library to obtain specific GAG structures and conjugate them to fluorophores and sensorchips for analysis using strain-catalyzed click chemistry (Paper IV and Paper VI).

Indeed, we can use xylosides as tools to investigate and also utilize GAG biosynthesis. The answers we found in the work of this thesis open up new areas of investigation.

Since we found a very efficient inhibitor of β4GalT7, we could use it as a potent tool for investigating GAG biochemistry. For instance, we could administer such an inhibitor to cancer cells and observe how it affects cell proliferation or immune system recognition. We could also try to improve the structure of the inhibitor to make it even more efficient.

Also, we can use the azide-containing xyloside to answer questions regarding the GAG expression of different cell types and how the types of GAGs might affect pathogens such as SARS-CoV-2. For example, we could utilize the azide-containing xylosides with the GAGome to create microarrays to find more exact epitopes where the pathogen could interact. Alternatively, we could administer azide-containing xylosides to cells from clinically obtained samples, modify them with a suitable extension, and compare them with similarly obtained xyloside-GAGs from healthy cell lines. There are many possibilities to consider.

With this expanded toolbox of modified xylosides, there is no doubt we can use them to answer more questions regarding GAG biosynthesis and glycobiology.

References

(1) Nealson, K. H.; Hastings, J. W. *Microbiol. Rev.* **1979**, *43*, 496–518.

(2) Miller, M. B.; Bassler, B. L. *Annu. Rev. Microbiol.* **2001**, *55*, 165–199.

(3) Laine, R. A. *Glycobiology* **1994**, *4*, 759–767.

(4) Dwek, R. A. *Biochem. Soc. Trans.* **1995**, *23*, 1–25.

(5) Möckl, L. *Front. Cell Dev. Biol.* **2020**, *8*, 253.

(6) Kannagi, R.; Izawa, M.; Koike, T.; Miyazaki, K.; Kimura, N. *Cancer Sci.* **2004**, *95*, 377–384.

(7) Pinho, S. S.; Reis, C. A. *Nat. Rev. Cancer* **2015**, *15*, 540–555.

(8) Taylor, M. E.; Drickamer, K.; Schnaar, R. L.; Etzler, M. E.; Varki, A., *Discovery and Classification of Glycan-Binding Proteins*, 2015.

(9) Prado Acosta, M.; Lepenies, B. *Biochem. Soc. Trans.* **2019**, *47*, 1569–1579.

(10) Schnaar, R. L. *Arch. Biochem. Biophys.* **2004**, *426*, 163–172.

(11) Schnaar, R. L. *J. Leukoc. Biol.* **2016**, *99*, 825–38.

(12) Sharon, N. *Pure Appl. Chem.* **1988**, *60*, 1389–1394.

(13) Fischer, G.; Boedeker, C. *Ann. der Chemie und Pharm.* **1861**, *117*, 111–118.

(14) Lindahl, U.; Couchman, J.; Kimata, K.; Esko, J. D., *Proteoglycans and Sulfated Glycosaminoglycans*, 2015.

(15) DeAngelis, P. L.; Weigel, P. H. *Biochemistry* **1994**, *33*, 9033–9039.

(16) Yannas, V. *Biomater. Sci. - An Introd. to Mater. Med. Classes* **2004**, 127–136.

(17) Owens, R. T.; Wagner, W. D. *Arterioscler. Thromb. A J. Vasc. Biol.* **1991**, *11*, 1752–1758.

(18) Gulberti, S.; Lattard, V.; Fondeur, M.; Jacquinet, J.-C.; Mulliert, G.; Netter, P.; Magdalou, J.; Ouzzine, M.; Fournel-Gigleux, S. *J. Biol. Chem.* **2005**, *280*, 1417–1425.

(19) Koike, T.; Izumikawa, T.; Tamura, J.-I.; Kitagawa, H. *Biochem. J.* **2009**, *421*, 157–162.

(20) Sugahara, K.; Yamada, S.; Yoshida, K.; De Waard, P.; Vliegenthart, J. F. *J. Biol. Chem.* **1992**, *267*, 1528–1533.

(21) Sugahara, K.; Tohno-oka, R.; Yamada, S.; Khoo, K. H.; Morris, H. R.; Dell, A. *Glycobiology* **1994**, *4*, 535–544.

(22) Mizumoto, S.; Ikegawa, S.; Sugahara, K. *J. Biol. Chem.* **2013**, *288*, 10953–10961.

(23) Götte, M.; Kresse, H. *Biochem. Genet.* **2005**, *43*, 65–77.

(24) Seidler, D. G.; Faiyaz-Ul-Haque, M.; Hansen, U.; Yip, G. W.; Zaidi, S. H.; Teebi, A. S.; Kiesel, L.; Götte, M. *J. Mol. Med.* **2006**, *84*, 583–594.

(25) Bui, C.; Talhaoui, I.; Chabel, M.; Mulliert, G.; Coughtrie, M. W.; Ouzzine, M.; Fournel-Gigleux, S. *FEBS Lett.* **2010**, *584*, 3962–3968.

(26) Rahuel-Clermont, S.; Daligault, F.; Piet, M. H.; Gulberti, S.; Netter, P.; Branlant, G.; Magdalou, J.; Lattard, V. *Biochem. J.* **2010**, *432*, 303–311.

(27) Almeida, R.; Levery, S. B.; Mandel, U.; Kresse, H.; Schwientek, T.; Bennett, E. P.; Clausen, H. *J. Biol. Chem.* **1999**, *274*, 26165–26171.

(28) Okajima, T.; Yoshida, K.; Kondo, T.; Furukawa, K. *J. Biol. Chem.* **1999**, *274*, 22915–22918.

(29) Tsutsui, Y.; Ramakrishnan, B.; Qasba, P. K. *J. Biol. Chem.* **2013**, *288*, 31963–31970.

(30) Michaelis, L.; Menten, M. L.; Goody, R. S.; Johnson, K. A. *Biochemistry* **1913**, *49*, 333–369.

(31) Johnson, K. A.; Goody, R. S. *Biochemistry* **2011**, *50*, 8264–8269.

(32) Reed, M. C.; Lieb, A.; Nijhout, H. F. *BioEssays* **2010**, *32*, 422–429.

(33) Kaiser, P. M. *J. Mol. Catal.* **1980**, *8*, 431–442.

(34) Pasek, M.; Boeggeman, E.; Ramakrishnan, B.; Qasba, P. K. *Biochem. Biophys. Res. Commun.* **2010**, *394*, 679–684.

(35) García-García, J. F.; Corrales, G.; Casas, J.; Fernández-Mayoralas, A.; García-Junceda, E. *Mol. Biosyst.* **2011**, *7*, 1312–1321.

(36) Daligault, F.; Rahuel-Clermont, S.; Gulberti, S.; Cung, M.-T.; Branlant, G.; Netter, P.; Magdalou, J.; Lattard, V. *Biochem. J.* **2009**, *418*, 605–614.

(37) Saliba, M.; Ramalanjaona, N.; Gulberti, S.; Bertin-Jung, I.; Thomas, A.; Dahbi, S.; Lopin-Bon, C.; Jacquinet, J.-C.; Breton, C.; Ouzzine, M.; Fournel-Gigleux, S. *J. Biol. Chem.* **2015**, *290*, 7658–7670.

(38) Talhaoui, I.; Bui, C.; Oriol, R.; Mulliert, G.; Gulberti, S.; Netter, P.; Coughtrie, M. W.; Ouzzine, M.; Fournel-Gigleux, S. *J. Biol. Chem.* **2010**, *285*, 37342–37358.

(39) Siegbahn, A.; Manner, S.; Persson, A.; Tykesson, E.; Holmqvist, K.; Ochocinska, A.; Rönnols, J.; Sundin, A.; Mani, K.; Westergren-Thorsson, G.; Widmalm, G.; Ellervik, U. *Chem. Sci.* **2014**, *5*, 3501–3508.

(40) Siegbahn, A.; Thorsheim, K.; Ståhle, J.; Manner, S.; Hamark, C.; Persson, A.; Tykesson, E.; Mani, K.; Westergren-Thorsson, G.; Widmalm, G.; Ellervik, U. *Org. Biomol. Chem.* **2015**, *13*, 3351–3362.

(41) Rini, J. M.; Leffler, H., *Carbohydrate recognition and signaling*, Second Edi; Elsevier Inc.: 2010; Vol. 1, pp 85–91.

(42) Robinson, H. C.; Brett, M. J.; Tralaggan, P. J.; Lowther, D. A.; Okayama, M. *Biochem. J.* **1975**, *148*, 25–34.

(43) Fritz, T. A.; Lugemwa, F. N.; Sarkar, A. K.; Esko, J. D. *J. Biol. Chem.* **1994**, *269*, 300–307.

(44) Abrahamsson, C. O.; Ellervik, U.; Eriksson-Bajtner, J.; Jacobsson, M.; Mani, K. *Carbohydr. Res.* **2008**, *343*, 1473–1477.

(45) Robinson, H. C.; Lindahl, U. *Biochem. J.* **1981**, *194*, 575–586.

(46) Sobue, M.; Habuchi, H.; Ito, K.; Yonekura, H.; Oguri, K.; Sakurai, K.; Kamohara, S.; Ueno, Y.; Noyori, R.; Suzuki, S. *Biochem. J.* **1987**, *241*, 591–601.

(47) Lugemwa, F. N.; Esko, J. D. *J. Biol. Chem.* **1991**, *266*, 6674–6677.

(48) Tran, V. M.; Victor, X. V.; Yockman, J. W.; Kuberan, B. *Glycoconj. J.* **2010**, *27*, 625–633.

(49) Tran, V. M.; Kuberan, B. *Bioconjug. Chem.* **2014**, *25*, 262–268.

(50) Johnsson, R.; Mani, K.; Cheng, F.; Ellervik, U. *J. Org. Chem.* **2006**, *71*, 3444–3451.

(51) Holmqvist, K.; Persson, A.; Johnsson, R.; Löfgren, J.; Mani, K.; Ellervik, U. *Bioorg. Med. Chem.* **2013**, *21*, 3310–3317.

(52) Kuberan, B.; Ethirajan, M.; Victor, X. V.; Tran, V.; Nguyen, K.; Do, A. *ChemBioChem* **2008**, *9*, 198–200.

(53) Schwartz, N. B.; Roden, L. *J. Biol. Chem.* **1975**, *250*, 5200–5207.

(54) Fukunaga, Y.; Sobue, M.; Suzuki, N.; Kushida, H.; Suzuki, S.; Suzuki, S. *Biochim. Biophys. Acta - Gen. Subj.* **1975**, *381*, 443–447.

(55) Robinson, J. A.; Robinson, H. C. *Biochem. J.* **1981**, *194*, 839–846.

(56) Kolset, S. O.; Sakurai, K.; Ivhed, I.; Overvatn, A.; Suzuki, S. *Biochem. J.* **1990**, *265*, 637–645.

(57) Freeze, H. H.; Sampath, D.; Varki, A. *J. Biol. Chem.* **1993**, *268*, 1618–1627.

(58) Nguyen, T. K.; Tran, V. M.; Sorna, V.; Eriksson, I.; Kojima, A.; Koketsu, M.; Loganathan, D.; Kjellén, L.; Dorsky, R. I.; Chien, C. B.; Kuberan, B. *ACS Chem. Biol.* **2013**, *8*, 939–948.

(59) Raman, K.; Ninomiya, M.; Nguyen, T. K. N.; Tsuzuki, Y.; Koketsu, M.; Kuberan, B. *Biochem. Biophys. Res. Commun.* **2011**, *404*, 86–89.

(60) Siegbahn, A.; Aili, U.; Ochocinska, A.; Olofsson, M.; Rönnols, J.; Mani, K.; Widmalm, G.; Ellervik, U. *Bioorg. Med. Chem.* **2011**, *19*, 4114–4126.

(61) Tsuzuki, Y.; Nguyen, T. K. N.; Garud, D. R.; Kuberan, B.; Koketsu, M. *Bioorg. Med. Chem. Lett.* **2010**, *20*, 7269–7273.

(62) Garud, D. R.; Tran, V. M.; Victor, X. V.; Koketsu, M.; Kuberan, B. *J. Biol. Chem.* **2008**, *283*, 28881–28887.

(63) Lugemwa, F. N.; Sarkar, A. K.; Esko, J. D. *J. Biol. Chem.* **1996**, *271*, 19159–19165.

(64) Bellamy, F.; Barberousse, V.; Martin, N.; Masson, P.; Millet, J.; Samreth, S.; Sepulchre, C.; Theveniaux, J.; Horton, D. *Eur. J. Med. Chem.* **1995**, *30*, 101s–115s.

(65) GlaxoSmithKline, *https://www.clinicaltrials.gov/ct2/show/NCT00244725,* **2006**, accessed 2021-08–02.

(66) Masson, P. J.; Coup, D.; Millet, J.; Brown, N. L. *J. Biol. Chem.* **1995**, *270*, 2662–2668.

(67) Renaut, P.; Millet, J.; Sepulchre, C.; Theveniaux, J.; Barberousse, V.; Jeanneret, V.; Vogel, P. *Helv. Chim. Acta* **1998**, *81*, 2043–2052.

(68) Chicaud, P.; Rademakers, J.; Millet, J. *Pathophysiol. Haemost. Thromb.* **1998**, *28*, 313–320.

(69) Varki, A. *Glycobiology* **2017**, *27*, 3–49.

(70) Mani, K.; Havsmark, B.; Persson, S.; Kaneda, Y.; Yamamoto, H.; Sakurai, K.; Ashikari, S.; Habuchi, H.; Suzuki, S.; Kimata, K.; Malmström, A.; Westergren-Thorsson, G.; Fransson, L. A. *Cancer Res.* **1998**, *58*, 1099–104.

(71) Malmberg, J.; Mani, K.; Säwén, E.; Wirén, A.; Ellervik, U. *Bioorg. Med. Chem.* **2006**, *14*, 6659–6665.

(72) Skaanderup, P. R.; Poulsen, C. S.; Hyldtoft, L.; Jørgensen, M. R.; Madsen, R. *Synthesis (Stuttg).* **2002**, *2002*, 1721–1727.

(73) Andresen, T. L.; Skytte, D. M.; Madsen, R. *Org. Biomol. Chem.* **2004**, *2*, 2951–2957.

(74) Luchetti, G.; Ding, K.; D'Alarcao, M.; Kornienko, A. *Synthesis (Stuttg).* **2008**, 3142–3147.

(75) Kornienko, A.; D'Alarcao, M. *Tetrahedron Asymmetry* **1999**, *10*, 827–829.

(76) Whistler, R. L.; Van Es, T. *J. Org. Chem.* **1963**, *28*, 2303–2304.

(77) Collette, Y.; Ou, K.; Pires, J.; Baudry, M.; Descotes, G.; Praly, J. P.; Barberousse, V. *Carbohydr. Res.* **1999**, *318*, 162–166.

(78) Baudry, M.; Barberousse, V.; Descotes, G.; Faure, R.; Pires, J.; Praly, J. P. *Tetrahedron* **1998**, *54*, 7431–7446.

(79) Baudry, M.; Barberousse, V.; Collette, Y.; Descotes, G.; Pires, J.; Praly, J. P.; Samreth, S. *Tetrahedron* **1998**, *54*, 13783–13792.

(80) Baudry, M.; Barberousse, V.; Descotes, G.; Pires, J.; Praly, J. P. *Tetrahedron* **1998**, *54*, 7447–7456.

(81) Thorsheim, K.; Clementson, S.; Tykesson, E.; Bengtsson, D.; Strand, D.; Ellervik, U. *Tetrahedron Lett.* **2017**, *58*, 3466–3469.

(82) Ramakrishnan, B.; Ramasamy, V.; Qasba, P. K. *J. Mol. Biol.* **2006**, *357*, 1619–1633.

(83) Manner, S.; Ellervik, U. *Synlett* **2014**, *25*, 1271–1274.

(84) Barton, D. H.; McCombie, S. W. *J. Chem. Soc. Perkin Trans.* **1975**, *1*, 1574–1585.

(85) Crich, D.; Quintero, L. *Chem. Rev.* **1989**, *89*, 1413–1432.

(86) Shi, X. X.; Shen, C. L.; Yao, J. Z.; Nie, L. D.; Quan, N. *Tetrahedron Asymmetry* **2010**, *21*, 277–284.

(87) Ochocinska, A.; Siegbahn, A.; Ellervik, U. *Tetrahedron Lett.* **2010**, *51*, 5200–5202.

(88) Plé, K.; Chwalek, M.; Voutquenne-Nazabadioko, L. *European J. Org. Chem.* **2004**, 1588–1603.

(89) Plé, K.; Chwalek, M.; Voutquenne-Nazabadioko, L. *Tetrahedron* **2005**, *61*, 4347–4362.

(90) Ren, L.; Liu, Y. X.; Lv, D.; Yan, M. C.; Nie, H.; Liu, Y.; Cheng, M. S. *Molecules* **2013**, *18*, 15193–15206.

(91) Lemieux, R. U.; Driguez, H. *J. Am. Chem. Soc.* **1975**, *97*, 4069–4075.

(92) Deslongchamps, P.; Chênevert, R.; Taillefer, R. J.; Moreau, C.; Saunders, J. K. *Can. J. Chem.* **1975**, *53*, 1601–1615.

(93) King, J. F.; Allbutt, A. D. *Can. J. Chem.* **1970**, *48*, 1754–1769.

(94) Dahbi, S.; Jacquinet, J. C.; Bertin-Jung, I.; Robert, A.; Ramalanjaona, N.; Gulberti, S.; Fournel-Gigleux, S.; Lopin-Bon, C. *Org. Biomol. Chem.* **2017**, *15*, 9653–9669.

(95) Krzywinski, M. I.; Schein, J. E.; Birol, I.; Connors, J.; Gascoyne, R.; Horsman, D.; Jones, S. J.; Marra, M. A. *Genome Res.* **2009**, DOI: 10.1101/gr.092759.109.

(96) Krupička, M.; Tvaroška, I. *J. Phys. Chem. B* **2009**, *113*, 11314–11319.

(97) Grison, C.; Chibli, H.; Barthès, N.; Coutrot, P. *J. Org. Chem.* **2006**, *71*, 7978–7988.

(98) Weeks, M. H. H.; Musselman, N. P. P.; Yevich, P. P. P.; Jacobson, K. H. H.; Oberst, F. W. W. *Am. Ind. Hyg. Assoc. J.* **1964**, *25*, 470–475.

(99) Jones, G. H.; Taniguchi, M.; Tegg, D.; Moffatt, J. G. *J. Org. Chem.* **1979**, *44*, 1309–1317.

(100) Nilsson, U.; Johnsson, R.; Fransson, L.-Å.; Ellervik, U.; Mani, K. *Cancer Res.* **2010**, *70*, 3771–3779.

(101) Persson, A.; Tykesson, E.; Westergren-Thorsson, G.; Malmström, A.; Ellervik, U.; Mani, K. *J. Biol. Chem.* **2016**, *291*, 14871–14882.

(102) Nasir, W.; Toledo, A. G.; Noborn, F.; Nilsson, J.; Wang, M.; Bandeira, N.; Larson, G. *J. Proteome Res.* **2016**, *15*, 2826–2840.

(103) Victor, X. V.; Nguyen, T. K.; Ethirajan, M.; Tran, V. M.; Nguyen, K. V.; Kuberan, B. *J. Biol. Chem.* **2009**, *284*, 25842–25853.

(104) Veber, D. F.; Johnson, S. R.; Cheng, H.-Y.; Smith, B. R.; Ward, K. W.; Kopple, K. D. *J. Med. Chem.* **2002**, *45*, 2615–2623.

(105) Matsson, P.; Doak, B. C.; Over, B.; Kihlberg, J. *Adv. Drug Deliv. Rev.* **2016**, *101*, 42–61.

(106) Matsson, P.; Kihlberg, J. *J. Med. Chem.* **2017**, *60*, 1662–1664.

(107) Lipinski, C. A.; Lombardo, F.; Dominy, B. W.; Feeney, P. J. *Adv. Drug Deliv. Rev.* **1997**, *23*, 3–25.

(108) Leo, A.; Hansch, C.; Elkins, D. *Chem. Rev.* **1971**, *71*, 525–616.

(109) Johnsson, R.; Mani, K.; Ellervik, U. *Bioorg. Med. Chem. Lett.* **2007**, *17*, 2338–2341.

(110) Naganbabu, M.; Perkins, L. A.; Wang, Y.; Kurish, J.; Schmidt, B. F.; Bruchez, M. P. *Bioconjug. Chem.* **2016**, *27*, 1525–1531.

(111) Lee, M. M.; Peterson, B. R. *ACS Omega* **2016**, *1*, 1266–1276.

(112) Lee, M. M.; Gao, Z.; Peterson, B. R. *Angew. Chemie - Int. Ed.* **2017**, *56*, 6927–6931.

(113) Goyvaerts, V.; Van Snick, S.; D'Huys, L.; Vitale, R.; Helmer Lauer, M.; Wang, S.; Leen, V.; Dehaen, W.; Hofkens, J. *Chem. Commun.* **2020**, *56*, 3317–3320.

(114) Bhola, R. K.; Das, P. K.; Pradhan, S.; Chakraborty, K.; Mohapatra, D.; Samal, P.; Patra, P. C.; Panda, S. S.; Mishra, S. K. *J. Hematop.* **2020**, *13*, 13–24.

(115) Qu, J.; Kohl, C.; Pottek, M.; Müllen, K. *Angew. Chemie - Int. Ed.* **2004**, *43*, 1528–1531.

(116) De Halleux, V.; Mamdouh, W.; De Feyter, S.; De Schryver, F.; Levin, J.; Geerts, Y. H. *J. Photochem. Photobiol. A Chem.* **2006**, *178*, 251–257.

(117) Valkó, K.; Plass, M.; Bevan, C.; Reynolds, D.; Abraham, M. H. *J. Chromatogr. A* **1998**, *797*, 41–55.

(118) Valkó, K. *J. Chromatogr. A* **2004**, *1037*, 299–310.

(119) Lavis, L. D. Ester bonds in prodrugs, 2008.

(120) Jones, M. B.; Teng, H.; Rhee, J. K.; Lahar, N.; Baskaran, G.; Yarema, K. J. *Biotechnol. Bioeng.* **2004**, *85*, 394–405.

(121) Osby, J. O.; Martin, M. G.; Ganem, B. *Tetrahedron Lett.* **1984**, *25*, 2093–2096.

(122) Huang, D.; Yan, G. *Adv. Synth. Catal.* **2017**, *359*, 1600–1619.

Scientific publications